Interactive comment on "Estimating contributions from biomass burning and fossil fuel combustion by means of radiocarbon analysis of carbonaceous aerosols: application to the Valley of Chamonix" by L. Bonvalot et al.

Anonymous Referee #1

The authors would like to thank the Reviewer #2 for his/her careful reading and comments, which helped to clarify the manuscript.
The reviewer comments are written in black, our responses in blue and *changes to the manuscript in italic blue.*

General comments
The authors present a comprehensive evaluation and validation of the novel EA-GIS-AixMICADAS facility, used to measure radiocarbon without any prior graphitization. The method is also applied to real aerosol samples from the alpine Chamonix Valley. The authors prove the accuracy and precision of the method in a satisfactory manner. Further, great benefit with this facility and method compared to other accelerator mass spectrometers (AMS) is the fact that no graphitization of aerosol samples are needed prior AMS. This makes the method more cost and time efficient. From my experience with graphitization this also means that several errors and sample losses can be avoided.
The applicability to real aerosol samples from the Chamonix Valley show satisfactory results which are in line to what one can expect in terms of source impact during different seasons. The source apportionment model to calculate TC fractions of biogenic, biomass burning and fossil fuel combustion is presented in a clear and concise way and is easily applicable by other researchers for similar studies.
The language is on a clear and high level.

Specific comments

The title is in my opinion to broad and general. It does not say anything about the novel radiocarbon analysis without graphitization. Further, if the authors are about the mention sources in the title as "biomass burning" and "fossil fuel combustion", I am wondering why they don't mention biogenic carbon? This fraction has a considerable role in the results and discussion session in the paper. Finally, the sources were not solely determined by radiocarbon, I would say that levoglucosan was equally important, so why omit levoglucosan?
I recommend this manuscript to be published in ACP.

We have complemented the title with both levoglucosan and biogenic carbon.

Page 1, line 15. Please explain the abbreviation AixMICADAS, if not here in the abstract then the first time the abbreviation appears in the following text.
The AixMICADAS abbreviation is explained Page 3 Line 19. The manufacturer name is also stated there.
AixMICADAS is based on an updated version of the MICADAS (MIni CArbon DAting System) developed and constructed by the ETH Zurich and now produced by the company IonPlus. In contrast to conventional off-line solid AMS analyses where the sample preparation, i. e. graphitization, (Genberg et al., 2010, 2013) of very small samples is complex and time consuming, this method is now applied to very small samples (5-100 µgC) without complex preparation and handling problems.

Page 1, line 27. The unit is given in µg.m-3. Why a dot "." between µg and m-3, this appears several times in the text but is not consequent. Sometimes this unit is written without a dot between.
All the units have been rewritten without dot.

Page 2, line 17. Can you please give a number of how large the carbonaceous fraction of PM can be, this would give important knowledge and a feeling for the numbers in this field, especially for new readers.
Page 2, line 19. It has been added that at least a third of the PM are composed of carbonaceous compounds.

Page 2, line 21. It feels a bit arrogant to state that there are "obvious scientific and societal implications", I suggest that you erase the word "obvious".
Page 2, line 23. "Obvious" has been removed.

Page 2, line 20-26. Consider re-write this paragraph, it is a bit confusing. End with "ideal test site for such measurements". Which measurements? Those you are referring to in line 20?
Page 2, lines 27-29. The end of this paragraph has been rewritten. Now, it states:
Due to very limited exogenous contributions, notably during winter, the typology of aerosol sources remains simple, which constitute an ideal site for testing a new method of aerosol sources characterization.

Page 3, line 16. The AMS AixMICADAS, state its manufacturer and model name if possible.
Page 3 Line 19. The manufacturer has been added. So far, each MICADAS is a prototype with its own improvements (see Bard et al. 2015 *NIM* for AixMICADAS)

Page 3, line 17-18. Other studies have also shown to handle small samples 10-100 µgC with graphitization prior AMS (Genberg et al., 2010).
Page 3, lines 20-23. This reference has been added together with another one from the same group with a focus on aerosol samples (Genberg et al. 2013).
In contrast to conventional off-line solid AMS analyses where the sample preparation, i. e. graphitization, (Genberg et al., 2010, 2013) of very small samples is complex and time consuming, this method is now applied to very small samples (5-100 µgC) without complex preparation and handling problems.

Page 3, line 31. What do you mean by hybrid ion source? This it can both handle graphite targets and CO2 gas? Please clarify this.
Page 4, lines 5-6. Indeed, the hybrid ion source can handle graphite target and CO_2 gas. The sentence has been rewritten for clarification.
It is equipped with a hybrid ion source that can both handle graphite targets and CO_2 *gas*

Page 4, line 11. In what atmosphere are you heating the sample to evolve the CO2? This should be stated. Further it is a bit confusing in which temperature the CO2 is evolved, in 450°C or in 1050°C in the EA? Please clarify this.
Page 4, lines 15-18. The combustion of the sample in the EA and the CO_2 transfer process have been detailed.
The sample is oxidized in the combustion tube under an oxygen-helium atmosphere temporarily enriched with oxygen; the tungsten oxide bed supporting the complete oxidation of combustion gases. Then, the evolved CO_2*, water and nitrogen oxides flow through the reduction tube (helium is used as carrier gas) where nitrogen oxides are reduced as* N_2

Page 4, line 15. It is a bit confusing that you mention the sampled PM10 filters here prior to the paragraph regarding sampling of filters. Please consider putting the sampling paragraph before the AMS section.
Page 4, lines 22-23. We have thus changed the sentence to avoid mentioning the samples. We agree that mentioning the sampled PM_{10} filters of the Arve Valley in this paragraph was confusing, but moving entirely the sampling paragraph before the AMS section would have disrupted the separation between the method protocol (with "home-made" aerosols) and the analysis of the Arve Valley samples.
This conservative value is based on the average difference between several duplicate measurements of different aerosol samples.

Page 4, line 22. OxA2 is an abbreviation, please spell out the whole name of this standard.
Page 4, line 30. OxA2 stands for oxalic acid 2 standard. Its definition has been added.

Page 4, line 26. Why did you consider these 46 OxA2 gas samples as unknown samples when you obviously knew the F14C of this SRM?
Page 5, lines 2-4. These additional 46 OxA2 gas samples were considered as samples to measure the average and standard deviation. They are thus completely independent from the other OxA2 measurements, which are used for correction and normalization. This ensures that the mean and standard deviation can be used to assess the accuracy and precision of the AMS measurements (see Bard et al. 2015 NIM).
OxA2 gas samples are considered as unknown samples so they are not used to correct and normalize measurements (i.e. machine transmission and chemistry fractionation) (Bard et al., 2015) and SD can be quantify.

Page 4, line 33. ASN/AON. Please explain or omit this.
Page 5, line 9. We added:
A_{SN}/A_{ON} with A_{SN} the normalized specific activity of the sample and A_{ON} the normalized specific activity of the OxA2.

Page 5, line 11-14. I would say that the filter handling and preparation induces most contamination, do you have any reference saying that the silver boat induces large or substantial contamination?
Page 5, lines 24-26. The text has been complemented.
By using the EA, we previously quantified the carbon content of empty silver boats, resulting in a contamination on the order of 1-2 µgC per boat. Similar carbon contaminations have been quantified by Ruff et al. (2010b) for smaller tin boats.

Page 6, line 7. You should say that SRM stands for Standard Reference Material. This is not known to everyone.
Page 6, line 19. The SRM acronym is explained.

Page 6, line 10. What is AGE-3 system? Reference?
Page 6, lines 22-23. AGE-3 is the graphization system. The acronym is explained and a reference about this system has been added (Wacker, et al. 2010)

Page 8, line 7. DECOMBIO, abbreviation for what?
Page 8, lines 21-23. A definition of the aim of the DECOMBIO project has been added.
…which focuses on the source apportionment of PM_{10} in the Arve Valley, and the evolution of the contribution of biomass burning emissions (DEconvolution COMBustion BIOmass).

Page 8, line 10. Please be more specific on the sampling locations. Was it on roofs of buildings? Ground level? How close to the nearest road? Surrounding landscape? Mountains, forests, pastures etc?
Page 8, lines 26-29. Precisions about the sampling locations have been added.
The collection sites are presented in Fig. 4. Sampling in the city of Passy (12,000 inhabitants) was performed at 583 m asl (above sea level) whereas sampling in Chamonix (9,000 inhabitants) took place at 1035 m asl. For both sampling sites the PM collection occurs about 4 m above the ground. The Passy sampling station is located in a parking lot, 20 m of the closest house and 90 m of a road. The Chamonix sampling occured in the city center, close to shops.

Page 8, line 13. Did you prebake the quartz fiber filters to avoid contamination of VOC's prior sampling? What size of filter did you use? What was the brand and model of filters and sampler?
Page 8, line 30 – page 9, line 1. Precisions about the filters have been stated.
Daily PM_{10} samples were collected on quartz filter, using Digitel DA-80 High Volume Sampler (30 m^3 h^{-1}). All filters (quartz filters, Pall Tissu Quartz, 150 mm Ø) were pre-baked at 500 °C for 8 h. They were stored in aluminum foil, sealed in a polyethylene sheath before the PM sampling. After collection, filters were folded, wrapped in aluminum foils, sealed in polyethylene bags and stored at -20°C.

Page 8, line 18. HPLC-PAD, abbreviation for what?
Page 9, lines 6-7. The full technique name is stated.
… High Performance Liquid Chromatography coupled with Pulsed Amperometric Detection (Dionex, HPLC DX500 and PAD ED40)

Page 8, line 22. Please state the brand and model of the TOA.
Page 9, lines 11-12. The brand of the TOA is added.
…by thermal-optical analysis (TOA) EUSAAR2 (Cavalli et al., 2010) with a Sunset apparatus (Birch and Cary, 1996).

Page 8, line 23. Please state the brand and model of the TEOM-FDMS.
Page 9, lines 12-13. Brand and model of TEOM and FDMS is added.
(TEOM 1400 ab and FDMS 8500c from Thermo Scientific)

Page 9, line 4. Please explain the abbreviation LGGE.
Page 9, lines 26 and 28. LGGE and CEREGE are lab names, as listed in the authors affiliations. For clarity, the technique used is stated for each lab.
The carbon content data measured by TOA in the LGGE (Grenoble) and by the GIS in the CEREGE (Aix-en-Provence)…

Page 9, line 9. Please explain the abbreviation CEREGE.
Page 9, lines 26 and 28. LGGE and CEREGE are lab names, as listed in the authors affiliations. For clarity, the technique used is stated for each lab.
The carbon content data measured by TOA in the LGGE (Grenoble) and by the GIS in the CEREGE (Aix-en-Provence)…

Page 10, line 6. Please mention some meteorological conditions that may reduce photo-oxidation during winter.
Page 10, lines 26-27. We added in parenthesis that the reduction of daylight and strong presence of smog and clouds reduce the photo-oxidation.

Page 10, line 19. Please explain F14Cbio to the reader.

Page 11, lines 7-9. $F^{14}C_{atmo}$ is added for more clarity. $F^{14}C_{atmo}$ is deduced from the literature. As all living systems (like the biomass) exchange with the atmosphere, their radiocarbon level is the same. Therefore $F^{14}C_{atmo} = F^{14}C_{bio}$.

From these studies, the atmospheric value for the year 2013-2014 can be estimated to $F^{14}C_{atmo} = 1.04$*. Hence, biogenic emissions from these years will present the same value (*$F^{14}C_{atmo} = F^{14}C_{bio} = 1.04$*).*

Page 11, line 3-4. "For the summer season, it is considered that all non-fossil carbon originates from organic compounds naturally released by living plants". Is this consideration true? What about organic PM from charcoal BBQs? Forest fires?

Page 11, lines 23-26. The Arve Valley is not prone to wild fires, and none was recorded during the sampling period. Cholesterol has been quantified in nearly all the samples. This proxy is generally used to quantify the "cooking" influence as it is emitted by cooking meat (charbroiling). The summer samples exhibit very low (often below detection limit) levels of cholesterol, confirming that the influence of meat charbroiling and therefore from BBQ and associated sources can be neglected. The following reference has been added: Schauer, et al. 1999.

No wild fire was recorded during the sampling period and the influence of the charcoal from barbecue cooking is neglected; levels of cholesterol, generally emitted by meat charbroiling (Schauer et al., 1999) remain very low, pointing that this cooking technique is not important here. Therefore, only the biogenic source of aerosols is considered, whose $F^{14}C$ *value should be close to the atmospheric value at the time of sampling (*$F^{14}C_{bio} = 1.04$*).*

Page 13, line 15. These F14C values and explanation should have been presented earlier in the manuscript. At page 10 for instance.

Page 14, line 7. The $F^{14}C_{bio}$ and $F^{14}C_{bb}$ values are now presented in the 3.2.1 paragraph.

Page 14, line 5-7. TCbb=TCNF-a*[levoglucosan]. To me, what you propose in this equation is the calculation of TCBio, i.e. TCBio=TCNF-a*[levoglucosan]. TCbb should be: TCbb=a*[levoglucosan], where a is the slope between TCNF and levoglucosan.

With the currently proposed formula, TCbb would be zero (0) during winter which seem highly unrealistic.

Page 14, lines 29-30. This was a cut and paste mistake. The equation we used is indeed: TC_{bb} = a x [levoglucosan]

Page 15, line 27. Instead of using LGGE and CERGE, which I assume are labs (?), I would prefer if you state the actually used method instead, i.e. EA and TOA. This would make more sense. Either way, you need to explain the abbreviations LGGE and CERGE, which currently are adding confusion to the manuscript.

Page 16, lines 29-20. Quantification methods have been added. The acronyms are lab names in French as used in the authors affiliations Rather than detailing the long acronyms, we added the town location for each laboratory.

Page 24, Table 1. "X modern carbon". Please state the unit of this parameter and explain it in the caption of the table.

Page 25, Table 1. The X modern carbon state for the mass fraction of modern carbon as defined in Eq. (5), and therefore has no unit. A small definition of the unit has been added in the caption of the table.

Page 25, Table 1. Which proportions of each SRM did you use in the mixture?

Page 25, Table 1. Precision about the determination of X modern carbon has been added, so the reader can determine the SRMs proportions.

Mass fraction of each SRM can be calculated using their carbon content (i.e. 45% for SRM1 515 and 78 % for SRM 2975.

Page 24, Table 1. “Error”. What type of error is this? Should be stated.
Page 25, Table 1. It is now stated that it is a standard error.

Page 24, Table 1. “Measurement after graphitization”. Here should be a unit in this column.
Page 25, Table 1. The unit ($F^{14}C$) has been added.

Page 25, Table 2. “0.532 F14C”. Remove “F14C” as it is stated in the explaining column text.
Page 26, Table 2. $F^{14}C$ has been removed.

Page 26, Table 3. Please explain the “Winter fNF,ref=1.10 F14C=1.09 fM” that is stated in the table. Same for summer a couple of rows further down. These should be explained in the table caption.
Page 27, Table 3. These values are now explained in the caption.
For winter, it is considered that all the non-fossil carbon originates from biomass burning (i.e. $f_{NF,ref}= F^{14}C_{bb}$) whereas all the non-fossil carbon during summer is assumed to originate from biogenic emissions (i.e. $f_{NF,ref}= F^{14}C_{bio}$). The reference values ($f_{NF,ref}$) for winter and summer are expressed in $F^{14}C$ f_M. Fossil and non-fossil fractions (f_F and f_{NF}) are determined by the radiocarbon measurements (see Eq. (6))

Page 26, Table 3. Column “± Carbon mass [µg.m-3]”. Please state the type of uncertainty, SD, SE, CI?
Page 27, Table 3. The type of uncertainty is now stated (CI).

Page 27, Table 4. Please state the type of uncertainty, SD, SE, CI?
Page 28, Table 4. It is now stated in the caption that uncertainties are confidence intervals.

Page 28, Table 5. Please state the type of uncertainty, SD, SE, CI?
Page 29, Table 5. It is now stated in the caption that uncertainties are confidence intervals.

Page 29, Table 6. First row, first column. Write “Date”.
Page 30, Table 6. “Date” has been added.

Page 29, Table 6. Please state the type of uncertainty, SD, SE, CI?
Page 30, Table 6. The type of uncertainty is stated.
The uncertainties represent the confidence intervals (95 %), and are determined by uncertainties propagation.

Page 30, Figure 1. Please explain PA, Oxa2, MM and MS in the figure caption.
Page 31, Figure 1. All definitions are stated in the caption.

Page 31, Figure 2. Please explain what you mean by “simulated” in the figure caption. From where have you derived the “Theoretical F14C”, explain. Should further be stated in the figure caption that this graph includes measurements of SRM’s.
Page 32, Figure 2. The caption is rewritten for clarification. The test aerosols and theirs compositions are defined as well as the theoretical $F^{14}C$.
$F^{14}C$ values of synthetic and standard (test) aerosol samples measured with the gas source compared with theoretical values. These test aerosols are made of two Standard Reference Materials (SRM 2975 and SRM 1515). The compositions of the different mixtures are listed in Table 1 with the corresponding theoretical and measured $F^{14}C$.

Page 33, Figure 3. "Blue ribbon", looks green to me. "A large scatter is exhibit which can be caused by…." This sentence sounds erroneous.
Page 34, Figure 3.The color of the ribbon has been changed: a brighter blue is used.
The sentence has been modified:
The large scatter could be linked to heterogeneous loading during the production of RM 8785 as mentioned by Cavanagh & Watters (2005).

Page 34, Figure 5. State that you are comparing EA-GIS and TOA instead of LGGE and CEREGE.
Page 35, Figure 5. The figure and its caption have been updated with measurement methods and lab locations.

Page 35, Figure 6. Use "TC" or "Carbon Concentration" on the y-axis? Consistency.
Page 36, Figure 6. The figure has been changed. TC and [µgC m^{-3}] are now stated.

Technical corrections
Page 5, line 16. Parenthesis error.
Page 5, line 29. The parenthesis is corrected.

Page 13, line 23. Change "TableTable 5" to "Table 5".
Page 14, line 15. The typo is corrected.

Page 14, line 7. Change "[levoglocosan]" to "[levoglucosan]".
Page 14, line 30. The typo is corrected.

Page 25, Table 2. The font is not consistent in the table.
Page 26, Table 2. The font of the table is homogenized.

Page 27, Table 4. Change "masse" to "mass".
Page 28, Table 4. Mass is corrected.

Whole document: Please be consistent whether you use µgC or just µg. There are discrepancies throughout the whole document, in the tables and figures.
µgC is used for carbon mass and µg for other compounds mass.

Whole document: Please be consistent whether you use [µg.m-3] or [µg m-3], same error can be found in ng (nanograms). Personally, I don't see why you use a dot in between. There are discrepancies throughout the whole document, in the tables and figures.
The notation without dot is now used in the whole document.

References
Genberg, J., Stenstrom, K., Elfman, M., and Olsson, M.: DEVELOPMENT OF GRAPHITIZATION OF mu g-SIZED SAMPLES AT LUND UNIVERSITY, Radiocarbon, 52, 1270-1276, 2010.

The reference is added to the bibliography.

Added references

Birch, M. E. and Cary, R. A.: Elemental Carbon-Based Method for Monitoring Occupational Exposures to Particulate Diesel Exhaust, Aerosol Sci. Technol., 25(3), 221–241, doi:10.1080/02786829608965393, 1996.

Genberg, J., Stenström, K., Elfman, M. and Olsson, M.: Development of graphitization of μ-sized samples at Lund University, Radiocarbon, 52(2–3), 1270–1276, 2010.

Genberg, J., Perron, N., Olsson, M. and Stenstrom, K.: Sealed glass tube combustion of μg-sized aerosol samples, Radiocarbon, 55(2–3), 617–623, 2013.

Schauer, J. J., Kleeman, M. J., Cass, G. R. and Simoneit, B. R. T.: Measurement of Emissions from Air Pollution Sources. 3. C1−C29 Organic Compounds from Meat Charbroiling, Environ. Sci. Technol., 33(10), 1566-1577, doi: 10.1021/es980076j, 1999.

Wacker, L., Němec, M. and Bourquin, J.: A revolutionary graphitisation system: Fully automated, compact and simple, Nucl. Instrum. Methods Phys. Res. Sect. B Beam Interact. Mater. At., 268(7–8), 931–934, doi:10.1016/j.nimb.2009.10.067, 2010.

Interactive comment on “Estimating contributions from biomass burning and fossil fuel combustion by means of radiocarbon analysis of carbonaceous aerosols: application to the Valley of Chamonix” by Lise Bonvalot et al.

Anonymous Referee #3

Received and published: 6 July 2016

Identification and quantification of the carbon contribution to particulate matter (PM) is crucial for several aspects, such as health, climate and environmental policies. Radiocarbon analysis combined with organic tracers has been demonstrated to be a powerful tool to disentangle modern (e.g. biomass burning) from fossil carbon sources in PM. This paper excels in several aspects from previous work: (1) The newly introduced combination of directly coupled EA to a CO2 gas source of an AMS ion source results in high throughput of very small (10..100 ug) samples, circumventing the costly and time-consuming graphite step. (2) The measurement techniques, including a suite of reference standards and the important assessment of contamination (regarding the small sample size) are presented in full detail. (3) Due to the exceptionally high sample size and temporal resolution a detailed evaluation of source components of PM in two Alpine valleys is possible and presented convincingly in the paper. I recommend publication in acp without modification.

We thank the Anonymous Referee #3 for his/her comment underlining the strongest points of our paper.

Interactive comment on “Estimating contributions from biomass burning and fossil fuel combustion by means of radiocarbon analysis of carbonaceous aerosols: application to the Valley of Chamonix” by Lise Bonvalot et al.

S. Preunkert
preunkert@lgge.obs.ujf-grenoble.fr
Received and published: 8 August 2016

This study presents PM_{10} aerosol data obtained in summer and winter in a valley of the French Alps. Among others, a source apportionment study has been made with the aim to distinguish sources as fossil fuel, biomass burning and biogenic emissions on the base of ^{14}C measurements and levoglucosan. This revealed that summer samples exhibit an important relative contribution of non-fossil sources and a dominant contribution of biomass burning in winter. Interestingly, this very valuable data set and its important conclusions are similar to what was obtained in two source apportionment studies (Gelencsér et al., 2007; May et al., 2009) made on the basis of a two year round data set sampled on a weekly basis at five rural/remote sites in Europe. These detailed literature data set reflects atmospheric conditions of 2002/2003 on a European west east transect at altitudes from 40 to 3100 m asl. Given the fact that the source apportionment calculations were very similar than ins this study here, i.e. including also ^{14}C and levoglucosan measurements to distinguish fossil, biomass burning and biogenic emissions, it might be worth that the authors have a look on this dataset and benefit by comparing their new results with these existing literature data.

References:
Gelencsér, A., B. May, D. Simpson, A. Sánchez-Ochoa, A. Kasper-Giebl, H. Puxbaum, A. Caseiro, C. Pio, and M. Legrand (2007), Source apportionment of PM2.5 organic aerosol over Europe: Primary/secondary, natural/anthropogenic, and fossil/biogenic origin, J. Geophys. Res., 112, D23S04, doi:10.1029/2006JD008094.
MAY, B., WAGENBACH, D., HAMMER, S., STEIER, P., PUXBAUM, H. and PIO, C. (2009), The anthropogenic influence on carbonaceous aerosol in the European back- ground. Tellus B, 61: 464–472. doi:10.1111/j.1600-0889.2008.00379.x

We thank Dr. Preunkert for her advice about two other papers on ^{14}C in aerosols (Gelencser et al. 2007, May et al. 2009).

These papers published in 2007 and 2009, are based on similar apportionment calculations as in Szidat et al. (2004, 2006) already cited in our paper.

Both papers cited by Dr. Preunkert are based on the same ^{14}C analyses of pooled $PM_{2.5}$ aerosol samples for five European sites. Pooling aerosol filters reduces the number of ^{14}C analyses and allows to reach the necessary carbon amount to perform classical AMS analyses on graphite targets. Consequently, each site is only characterized by two values, one for winter and the other for summer (cf. Table 2 in Gelencsér et al. 2007, and the modified version as Table 1 in May et al. 2009).

In those papers the source apportionment is then based on the assumption of constant emission factors, e.g. OC_{bb}/levo and OC_{bb}/EC_{bb} from the literature, notably based on test combustion in experimental fireplaces and oven.

By contrast to former works based on a few ^{14}C analyses, our precise study of two close sites relies on more that one hundred of ^{14}C analyses (duplicates of more than 50 samples), which allows to evaluate the correlation between TC, levoglucosan and ^{14}C in many filters even characterized by low carbon contents (thanks to the low blank and detection limit reached with the gas ion source coupled to AixMICADAS).

Based on the observed linear relationship (our Fig. 7) we were able to calculate a non-fossil carbon/levoglucosan ratio independent from the literature on test combustion. As underlined in section 3.2 of our paper, the non-fossil carbon/levoglucosan ratio derived for Passy and Chamonix is compatible with the large range reported by Schmidl et al. (2008) for test combustion on various types of wood. Our value is also compatible with the central value and range assumed by Gelencser et al. (2007) and May et al. (2009) from the literature on test combustion. As noted in our paper, our measured value based on the dual radiocarbon-levoglucosan approach agrees very well with those obtained by Zotter et al. (2014) for several Swiss stations.

As far as the apportionment calculation is concerned, the novelty of our approach (section 3.2.3) is to propose to use the ratio derived from the numerous pairs of ^{14}C and levoglucosan measurements, instead of relying on an assumed and uncertain emission factor.

Estimating contributions from biomass burning, fossil fuel combustion and biogenic carbon to carbonaceous aerosols in the Valley of Chamonix: a dual approach based on radiocarbon and levoglucosan.

Lise Bonvalot[1], Thibaut Tuna[1], Yoann Fagault[1], Jean-Luc Jaffrezo[2], Véronique Jacob[2], Florie Chevrier[2,3], Edouard Bard[1]

[1]CEREGE, Aix-Marseille University, CNRS, IRD, Collège de France, Technopôle de l'Arbois, BP 80, 13545 Aix-en-Provence, France
[2]Université Grenoble Alpes / CNRS, LGGE-UMR 5183, F-38402, Saint Martin d'Hère
[3]Université Savoie Mont-Blanc – LCME, F-73376 Le Bourget du Lac Cedex

Correspondence to: Lise Bonvalot (bonvalot@cerege.fr); Edouard Bard (bard@cerege.fr)

Abstract. Atmospheric particulate matter (PM) affects the climate in various ways and has a negative impact on human health. In populated mountain valleys from Alpine regions, emissions from road traffic contribute to carbonaceous aerosols, but residential wood burning can be another source of PM during the winter.

We determine the contribution of fossil and non-fossil carbon sources by measuring radiocarbon in aerosols using the recently installed AixMICADAS facility. The accelerator mass spectrometer is coupled to an elemental analyzer (EA) by means of a gas interface system directly connected to the gas ion source. This system provides rapid and accurate radiocarbon measurements for small samples (10-100 µgC) with minimal preparation from the aerosol filters. We show how the contamination induced by the EA protocol can be quantified and corrected for. Several standards and synthetic samples are then used to demonstrate the precision and accuracy of aerosol measurements over the full range of expected $^{14}C/^{12}C$ ratios ranging from modern carbon to fossil carbon depleted in ^{14}C.

Aerosols sampled in Chamonix and Passy (Arve Valley, French Alps) from November 2013 to August 2014 are analyzed for both radiocarbon (124 analyses in total) and levoglucosan, which is commonly used as a specific tracer for biomass burning. NO_X concentration, which is expected to be associated with traffic emissions, is also monitored.

Based on ^{14}C measurements, we can show that the relative fraction of non-fossil carbon is significantly higher in winter than in summer. In winter, non-fossil carbon represents about 85 % of total carbon, while in summer this proportion is still 75 % considering all samples. The largest total carbon and levoglucosan concentrations are observed for winter aerosols with values up to 50 and 8 µg m^{-3}, respectively. These levels are higher than those observed in many European cities, but are close to those for other polluted Alpine valleys.

The non-fossil carbon concentrations are strongly correlated with the levoglucosan concentrations in winter samples, suggesting that almost all of the non-fossil carbon originates from wood combustion used for heating during winter.

For summer samples, the joint use of ^{14}C and levoglucosan measurements leads to a new model to quantify separately the contributions of biomass burning and biogenic emissions in the non-fossil fraction. The comparison of the biogenic fraction with polyols (a proxy for primary soil biogenic emissions) and with the temperature suggests a major influence of the secondary biogenic aerosols.

Significant correlations are found between the NO_X concentration and the fossil carbon concentration for all seasons and sites, confirming the relation between road traffic emissions and fossil carbon.

Overall this dual approach combining radiocarbon and levoglucosan analyses strengthens the conclusion concerning the impact of biomass burning. Combining these geochemical data both serves to detect and quantify additional carbon sources. The Arve Valley provides a first illustration of this model to aerosols.

1 Introduction

Airborne particles, generally known as atmospheric aerosols or particulate matter (PM), are the focus of many environmental concerns. Indeed, airborne particles affect the climate on a regional (Penner et al., 1998; Chung and Seinfeld, 2002) and global (Ramanathan et al., 2001a, 2001b) scale by modifying clouds properties (Jacobson et al., 2000), by reflecting, scattering and absorbing sunlight. Notably, the black carbon fraction of PM leads to the second largest anomaly of radiative forcing observed since the beginning of the industrial era, close behind anthropogenic CO_2 (Bond et al., 2013).

In addition, the harmful impact of PM on human health is well established: exposure to aerosols can cause respiratory and cardiopulmonary diseases that lead to increased mortality (Jerrett et al., 2005; Pope and Dockery, 2006; Kennedy, 2007; Lelieveld et al., 2015).

Carbonaceous particles constitute a major fraction (at least a third) of PM (Putaud et al., 2004, 2010). Their sources can be both biogenic and anthropogenic, leading to primary particles (i.e. directly emitted) and to secondary organic particles from gaseous precursors such as volatile organic compounds (Pöschl, 2005).

Improving the characterization of the relative contributions of anthropogenic and natural sources to PM is a crucial issue which has scientific and societal implications (Gustafsson et al., 2009). The importance in PM emission due to biomass burning (BB) for domestic heating has been shown for many urban areas (Jordan et al., 2006b; Zotter et al., 2014). The Arve Valley, located in the French Alps, is strongly impacted by pollution events and high PM concentrations. The severity of these events is due to a combination of topography and local meteorology, notably with temperature inversion layers during winter which trap air masses close to the ground (Herich et al., 2014). Due to very limited exogenous contributions, notably during winter, the typology of aerosol sources remains simple, which constitute an ideal site for testing a new method of aerosol sources characterization.

The pollution of the Arve valley has already been investigated with various techniques and results suggest the influence of local sources of carbon, more specifically from biomass burning used for residential heating during winter (Marchand et al., 2004; Aymoz et al., 2007; Herich et al., 2014). Different sources apportionment models (CMB/PMF/aethalometer) have been used to determine contribution of the biomass burning in a French alpine city (Grenoble) (Favez et al., 2010) but significant discrepancies due to differences in the conceptual hypotheses made for each model are still observed.

Radiocarbon (^{14}C) measurement of the carbonaceous PM fraction has been demonstrated as an effective tool for aerosol source apportionment, in particular for distinguishing fossil fuel combustion products from other carbon sources such as biomass burning and biogenic emissions (Jordan et al., 2006b; Szidat et al., 2006; El Haddad et al., 2011; Liu et al., 2013).

^{14}C is produced naturally in the upper atmosphere by the interaction of secondary neutrons from cosmic rays with nitrogen atoms. It is then oxidized into $^{14}CO_2$ and well mixed in the atmosphere before being partly taken up by vegetation during photosynthesis. Living organisms such as trees exhibit $^{14}C/^{12}C$ ratios similar to that of the atmospheric pool on the order of 10^{-12}.

Biomass fuel is defined as a generic term meaning a source of modern carbon. Several factors cause the atmospheric $^{14}C/^{12}C$ ratio to vary slightly from year to year, and this has been well documented over the last decades (Levin and Kromer, 2004; Hua et al., 2013; Levin et al., 2013). As a consequence, the $^{14}C/^{12}C$ ratio in the biomass will also vary with the year of growth. By contrast, fossil fuels are depleted in ^{14}C as they are made of sedimentary organic matter, which is much older than the radioactive half-life of ^{14}C ($T_{1/2}$ = 5730 years). Therefore, by measuring the ^{14}C in the whole carbonaceous fraction of aerosol samples, it is possible to quantify the fossil (f_F) and non-fossil (f_{NF}) fractions.

The direct coupling of an elemental analyzer (EA) to an accelerator mass spectrometer (AMS) is a fast and efficient way to measure the ^{14}C in small samples and, more particularly, in aerosols (Ruff et al., 2010a; Salazar et al., 2015). In our case, the CO_2 produced by combustion in the EA is delivered into the gas ion source of the AMS AixMICADAS (Bard et al., 2015) by means of the gas interface system (GIS) (Wacker et al., 2013). AixMICADAS is based on an updated version of the MICADAS (MIni CArbon DAting System) developed and constructed by the ETH Zurich and now produced by the company IonPlus. In contrast to conventional off-line solid AMS analyses where the sample preparation, *i. e.* graphitization, (Genberg et al., 2010, 2013) of very small samples is complex and time consuming, this method is now applied to very small samples (5-100 µgC) without complex preparation and handling problems. In the case of atmospheric PM samples, such a low required mass allows complementary analyses of other parameters on the same filter.

This study describes our protocol of PM sample analysis for ^{14}C, including the analyses of standards and blanks in order to quantify and correct for possible contamination (Ruff et al., 2010b). As an example of application, we then determine the fractions of fossil and non-fossil carbon in carbonaceous aerosols from the Arve Valley (French Alps), sampled in the cities of Passy and Chamonix, from November 2013 to August 2014. Levoglucosan, which is a biomass burning molecular proxy (Simoneit et al., 1999), is measured in the same samples and is used to provide an independent view of the biomass burning contribution. NO_X levels are also monitored in parallel, because they are mainly associated with traffic emissions. Polyols are measured as a proxy for primary biogenic aerosol particles.

2 Materials and methods

2.1 Radiocarbon measurements: method development

2.1.1 EA-GIS-AixMICADAS coupling

AixMICADAS is a compact AMS system dedicated to ^{14}C measurements in ultra-small samples (Synal et al., 2007; Bard et al., 2015). It operates at around 200 kV with carbon ion stripping in helium gas. It is equipped with a hybrid ion source that can both handle graphite targets and CO_2 gas (Fahrni et al., 2013; Wacker et al., 2013). It is coupled to a versatile gas interface system that ensures stable gas measurements from different sources: a cracker for CO_2 in glass ampoules, an automated system to handle carbonate, and an elemental analyzer for combusting organic matter. AixMICADAS and its performances are described elsewhere (Bard et al., 2015).

Atmospheric PM is collected on quartz filters, but only a small punch (between 0.2 and 1.5 cm^2, depending of the filter loading) is required for the ^{14}C analysis. The small filter punch is wrapped into a metallic boat before being combusted in the elemental analyzer. The sample preparation is carried out in a laminar flow hood to minimize contamination. The boats are made of silver (10x10x20 mm, about 240 mg each) and are baked at 800 °C for 2 hours to eliminate organic contamination. The EA (VarioMicroCube, Elementar) is equipped with a combustion tube filled with tungsten oxide granules (heated at 1050°C) and a reduction tube filled with copper wires and silver wool (heated at 550°C). The sample is oxidized in the combustion tube under an oxygen-helium atmosphere temporarily enriched with oxygen; the tungsten oxide bed supporting the complete oxidation of combustion gases. Then, the evolved CO_2, water and nitrogen oxides flow through the reduction tube (helium is used as carrier gas) where nitrogen oxides are reduced as N_2. A phosphorus pentoxide trap is then used to retain water produced during combustion and only the CO_2 is transferred and focused into the zeolite trap of the GIS. CO_2 is released by heating the trap to 450°C and is then transferred into the injection syringe by gas expansion. The CO_2 is quantified before addition of helium to obtain a 5% CO_2 mixture, which is finally injected into the ion source of AixMICADAS. An overall confidence interval of 4 % is considered for the carbon measurements. This conservative value is based on the average difference between several duplicate measurements of different aerosol samples. This 4 % value thus includes the intrinsic uncertainty of the measurement by the GIS, together with the additional uncertainty linked to loading heterogeneities at the surface of the filters and to the difficulty in punching exactly the same surface of the filter. This 4 % uncertainty is propagated to all values related to the carbon mass.

Measured $^{14}C/^{12}C$ ratios are corrected for fractionation based on the analysis of the ^{13}C ion beam on an AixMICADAS Faraday cup. ^{14}C data are then expressed as a normalized activity $F^{14}C$ ratio equivalent to Fraction Modern (Reimer et al., 2004).

Blank measurements are performed using CO_2 derived from fossil sources (without ^{14}C). Measurements of CO_2 produced from oxalic acid 2 standard (OxA2, National Institute of Standards and Technology, SRM 4990C) are used to normalize all $^{14}C/^{12}C$ ratios of the measured samples. Both blank and standard CO_2 are contained in bottles directly coupled to the GIS and its injection syringe. During 2015, 85 blank gas samples were measured, giving an average $F^{14}C$ of 0.0045 (SD = 0.0019, N = 85, and $\sigma_{er} = 0.0002$, $\sigma_{er}=SD/N^{1/2}$). This result is equivalent to a radiocarbon age of 43400 ± 360 years. During the same year, we added 46 OxA2 gas samples, considered as unknown samples, which led to an average $F^{14}C$ of 1.3405 (SD = 0.0064, N = 46, and σ_{er}= 0.0009). These values are compatible with the standard value of 1.3407 ± 0.0005 $F^{14}C$ (Stuiver, 1983). OxA2 gas samples are considered as unknown samples so they are not used to correct and normalize measurements (i.e. machine transmission and chemistry fractionation) (Bard et al., 2015) and SD can be quantify.

In aerosol science, the fraction of modern (f_M) is widely used. As underlined by Eriksson Stenström et al. (2011), it is not always clear if f_M has been corrected for decay since 1950 as in Currie et al. (1989). To avoid any confusion in our paper, all measurements will be expressed in $F^{14}C$ as defined by Reimer et al. (2004). $F^{14}C$ is defined as the ratio of the sample activity to the standard (OxA2) activity measured in the same year, with both activities background-corrected and $\delta^{13}C$ normalized (*i.e.* A_{SN}/A_{ON} with A_{SN} the normalized specific activity of the sample and A_{ON} the normalized specific activity of the OxA2). $F^{14}C$ does not depend on the year of measurement. Conversion between $F^{14}C$ and f_M (corrected for decay since 1950) is carried out following Eq. (1):

$$f_M = F^{14}C \times \exp\left[{}^{(1950 - T_m)}/_{8267}\right] \qquad (1)$$

with T_m the year of measurement and 8267 corresponding to the true mean life of radiocarbon expressed in years, i.e. the true half-life 5730 years divided by ln(2). The exponential factor is slightly lower than one, thus f_M is smaller than $F^{14}C$ (currently about 8 ‰). It is worth underlining that the non-fossil fraction f_{NF} and the fossil fraction f_F do not depend on the ^{14}C measurement unit. Indeed, f_{NF} and f_F are ratios between the sample measurement and a reference value, as detailed in Eq. (6), for the modern end-member (the fossil end-member staying at zero). As long as ^{14}C measurements and end-members values are expressed in the same unit ($F^{14}C$ or f_M), f_{NF} and f_F do not vary with the year of measurement and values determined at different times can be compared.

2.1.2 Contamination quantification

It is initially assumed that a sample of a carbon mass M_S and a $^{14}C/^{12}C$ ratio $F^{14}C_S$ analyzed with the EA-GIS coupling becomes contaminated with a constant mass of carbon M_C exhibiting a constant $^{14}C/^{12}C$ ratio $F^{14}C_C$. The main source of contamination is likely to come from the silver boat: while the heat treatment can remove the carbon adsorbed on metallic surfaces of the boat, carbon impurities occluded in the silver cannot be removed. By using the EA, we previously quantified the carbon content of empty silver boats, resulting in a contamination on the order of 1-2 µgC per boat. Similar carbon contaminations have been quantified by Ruff et al. (2010b) for smaller tin boats. Other sources of carbon may potentially originate in the preparation of the sample (filter) or even from EA-GIS coupling.

The ultimate contamination of metallic boats will be considered as constant. This assumption is expressed in the following mass balance equations Eq. (2) and Eq. (3) where M_M and $F^{14}C_M$ represent the measured mass and the measured isotopic ratio, respectively (Ruff et al., 2010a):

$$F^{14}C_M \times M_M = F^{14}C_S \times M_S + F^{14}C_C \times M_C \qquad (2)$$

$$M_M = M_S + M_C \tag{3}$$

In order to determine M_C and F_C and to test the assumption of constant values, blank and standard samples were measured with various masses M_M. Phthalic acid (PA) blank ($F^{14}C = 0$) and OxA2 standard were diluted in ultrapure water and various volumes (less than 25 µL) were deposited onto quartz filter (Pall Flex QAT) punch of approximately 1 cm^2 which had been prebaked at 500 °C for 2 hours. Spiked filters punches were wrapped in silver boats then loaded into the EA autosampler. Combining Eq. (2) and Eq. (3) leads to Eq. (4) in which the measured values M_M and $F^{14}C_M$ and the known $F^{14}C_S$ values are used to derive M_C and F_C of the contaminating carbon.

$$F^{14}C_M = \frac{(M_M - M_C)\times F^{14}C_S + M_C \times F^{14}C_C}{M_M} \tag{4}$$

OxA2 and PA samples with different carbon mass (M_M) were measured and a nonlinear weighted least squares method (weights corresponding to the measured uncertainties on $F^{14}C_M$ values) was applied to determine $F^{14}C_C$ and M_C. The results of the contamination model for the blank and the standard are represented in Fig. 1(a); the estimated parameters from the fit are $F^{14}C_C = 0.73 \pm 0.11$ and $M_C = 1.45 \pm 0.26$ µgC (95 % confidence interval). Figures 1(b) and 1(c) depict the same dataset corrected for the contamination parameters. It can be observed that $F^{14}C_S$ values for PA and Oxa2 are in agreement with the expected values confirming the constant contamination assumption. Contamination studies were also carried out without filter punches (the blank and standard are laid in solid forms in the silver boats), leading to similar contamination parameters. It may thus be deduced that the boats are the primary source of contamination.

2.1.3 Standard and synthetic aerosol samples

In order to mimic aerosol samples, two NIST standards were used as end-members and were mixed together to simulate different $^{14}C/^{12}C$ ratios: SRM (Standard Reference Material) 2975 Forklift Diesel Soot (78 % carbon) and SRM 1515 Apple Leaves (45% carbon). The first standard typifies fossil fuel combustion products while the second provides an analog of natural biopolymers generally found in PM (Currie and Kessler, 2005). $^{14}C/^{12}C$ ratios were determined by performing precise measurements on large samples of roughly 1 mgC that were graphitized with the AGE-3 system (Automated Graphitization Equipment, described in Wacker et al. (2010)) and analyzed with AixMICADAS using its hybrid ion source in the conventional mode. As expected, SRM 2975 exhibits a very low $^{14}C/^{12}C$ ratio ($F^{14}C = 0.0013$ with SD = 0.0002, N = 5, and $\sigma_{er} = 0.0001$, blank subtracted) whereas SRM 1515 has the $^{14}C/^{12}C$ ratio of the atmosphere at the time of its photosynthesis in 1985 ($F^{14}C = 1.1862$ with SD = 0.0017, N = 5, and $\sigma_{er} = 0.0007$).

Mixtures of the two SRM standards were prepared to obtain different $^{14}C/^{12}C$ ratios. To ensure homogeneity, the standards were mixed with an agate mortar and pestle. The relative proportion of modern carbon can be defined as follows in Eq. (5):

$$X_{modern\ carbon} = \frac{mC_{SRM1515}}{mC_{SRM1515} + mC_{SRM2975}} = \frac{0.45\times m_{SRM1515}}{0.45\times m_{SRM1515} + 0.78\times m_{SRM2975}} \tag{5}$$

Expected $F^{14}C$ values were calculated by using the mass of each SRM and their measured $F^{14}C$ as end-members. The uncertainties were calculated by propagating different sources of errors: the weighing uncertainty on the mass of each standard and the analytical uncertainties of the $^{14}C/^{12}C$ ratio of the pure standards. All mixed samples were graphitized with the AGE-3 system and measured with AixMICADAS (three measurements for each mixture). The small scatter of the results listed in Table 1 confirms that mixtures were well homogenized and that $^{14}C/^{12}C$ ratio determinations are reproducible. In addition, the good agreement between theoretical and measured values confirms that these mixtures can be used to simulate small aerosol samples.

Following this initial step, the SRM mixtures were loaded onto quartz filters. In order to simulate real aerosol samples, each powder mixture was suspended in ultrapure water. Different volumes of these suspensions (about 80 ngC mL^{-1}) were then deposited onto quartz filters that had been baked previously at 500 °C for 2h. A vacuum filtration system (Millipore) was used to eliminate most of the water and to distribute carbonaceous particles evenly over the filter surface. Loaded filters were dried overnight in a laminar airflow hood and then subsampled with a puncher (d = 11 mm / S = 0.95 cm^2) before being loaded into silver boats. Each standard mixture was measured at least four times with different carbon masses, corresponding to different loadings on independent filters. Mean results shown in Fig. 2 confirm the accuracy of aerosol measurements with the gas ion source over the full range of expected ^{14}C activities ($F^{14}C$ between 0.001 and 1.2).

To further test the precision and accuracy of the developed aerosol analytical procedures, we also analyzed two standards prepared from atmospheric particle matter (Table 2).

We acquired NIST SRM 1649b, prepared from the same bulk material as the original SRM 1649 and SRM 1649a (which are no longer available) but sieved to a smaller particle size fraction (63µm). The original bulk material, SRM 1649 was prepared at NIST from PM collected in 1976-77 in the Washington DC area over a 12-month period and issued in 1982 (Wise and Watters, 2007, 2009).

High precision measurements were performed to determine the $^{14}C/^{12}C$ ratio of NIST SRM 1649b. Samples were converted to graphite with the AGE 3 system. Four solid targets (≈ 1 mgC) were measured. On line gas measurements were also investigated using quartz filters loaded with NIST SRM 1649b. In short, SRM 1649b was suspended in ultrapure water (about 80 ngC mL^{-1}) and deposited onto previously baked quartz filters. Loaded filters were then dried in the clean hood, punched and wrapped into silver boats, ready for use with the EA-GIS coupled to AixMICADAS. The replicates (N = 7) were obtained with carbon mass ranging from 7 to 93 µgC.

Our graphite measurements of large samples are in agreement with the values reported in the literature for SRM 1649 and SRM 1649a(Currie et al., 1984; Currie et al., 2002; Szidat et al., 2004; Wise and Watters, 2007; Heal et al., 2011). The $F^{14}C$ value for the on line gas measurements is 0.505, with a SD of 0.028, N = 7, and a σ_{er} of 0.010, whereas the determined $F^{14}C$ for the solid measurements is 0.532 with a SD of 0.004, N = 4, and a σ_{er} of 0.002.

Two suggestions could be proposed to explain the small difference between solid and gaseous measurements. Some colloidal fraction or some water-soluble compounds may have been lost during sample preparation. If the soluble and insoluble fractions are of different origins, associated with different isotopic compositions, this could bias the $^{14}C/^{12}C$ ratio of the residual material loaded on the filter. Similarly, the ultrafine fraction (< 0.3 µm) not retained by the filter may have a different isotopic carbon composition, leading to the discrepancy between the solid and gaseous measurements.

Such a problem does not affect our results on mixtures of SRM 2975 and SRM 1515 standards described previously; indeed, these standards are more prone to be isotopically homogeneous because of their more simple composition as they are both originate from one source.

The second reference material is RM 8785, composed of the fraction lower than 2.5 µm (i.e. $PM_{2.5}$) of SRM 1649 which has been re-suspended in air and deposited onto quartz filters by NIST and SRI International (Cavanagh and Watters, 2005; Klouda et al., 2005). Analyses of three punches give an average $F^{14}C$ of 0.387 and SD of 0.08. This value is in agreement which measurements performed by five different laboratories (Szidat et al., 2013), even if it is positioned at the high end of the values (Fig. 3). Szidat et al. (2013) pointed out that $^{14}C/^{12}C$ results for RM 8785 exhibit a larger scatter than that measured on other PM samples during the same inter-comparison of laboratories. This was probably caused by heterogeneous loading during production of RM 8785 filters by NIST (concentrations ranging from 92 µg to 2855 µg onto 8.55 cm^2 (Cavanagh and Watters, 2005)) or to secondary deposition of volatile organic compounds (VOCs) onto the filters.

An additional source of $^{14}C/^{12}C$ scatter may be linked to the heterogeneity of fine particles (<2.5 µm) constituting RM 8785. Indeed, its average $F^{14}C$ value of approximately 0.39 is quite different from the value of approximately 0.5 measured for SRM 1649a, which was sieved at 125 µm only, and which is the raw material used to produce RM 8785. This suggests the possibility of isotopic heterogeneities between different particle sizes.

2.2 Samples from the Arve Valley

2.2.1 Sampling sites and procedures

The measurements were performed in the framework of the DECOMBIO program (Chevrier et al., 2016), which focuses on the source apportionment of PM_{10} in the Arve Valley, and the evolution of the contribution of biomass burning emissions (DEconvolution COMBustion BIOmass). Filters analyzed in our study were collected between November 2013 and August 2014 in Passy and between December 2013 and January 2014 in Chamonix. Both urban stations, maintained by the local Air Monitoring Agency (Air Rhône-Alpes) are located in the Arve Valley, in the French Alps. The collection sites are presented in Fig. 4. Sampling in the city of Passy (12,000 inhabitants) was performed at 583 m asl (above sea level) whereas sampling in Chamonix (9,000 inhabitants) took place at 1035 m asl. For both sampling sites the PM collection occurs about 4 m above the ground. The Passy sampling station is located in a parking lot, 20 m of the closest house and 90 m of a road. The Chamonix sampling occured in the city center, close to shops. Temperatures were monitored hourly at both sites throughout the sampling period. Daily PM_{10} samples were collected on quartz filter, using Digitel DA-80 High Volume Sampler (30 m^3 h^{-1}). All filters (quartz filters, Pall Tissu Quartz, 150 mm ∅) were pre-baked at 500 °C for 8 h. They were stored in aluminum foil, sealed in a polyethylene sheath before the PM sampling. After collection, filters were folded, wrapped in aluminum foils, sealed in polyethylene bags and stored at -20°C.

2.2.2 Additional data

Levoglucosan (1,6-anhydro-b-D-glucopyranose) is an anhydro-sugar, emitted by the pyrolysis of cellulose (Simoneit et al., 1999) and is widely used as a biomass burning tracer (Schauer et al., 2001; Jordan et al., 2006a; Caseiro et al., 2009). Here, the levoglucosan is water extracted and then quantified by High Performance Liquid Chromatography coupled with Pulsed Amperometric Detection (Dionex, HPLC DX500 and PAD ED40) (Waked et al., 2014). The concentrations of several polyols (arabitol, mannitol, sorbitol) are also determined by this analysis. Polyols at high concentration in the atmospheric PM are known to originate from emission from fungis from soils (Yttri et al., 2007; Bauer et al., 2008).

TC (total carbon) concentration is also quantified on the same filters by the determination of the EC (elemental carbon) and OC (organic carbon) by thermal-optical analysis (TOA) EUSAAR2 (Cavalli et al., 2010) with a Sunset apparatus (Birch and Cary, 1996). TC is equal to the sum of EC and OC. PM_{10} total mass is measured on line by TEOMS-FDMS (TEOM 1400 ab and FDMS 8500c from Thermo Scientific), taking into account the volatile and non-volatile fractions of the PM. NO_X ($NO+NO_2$) are also measured on line (with the Environnement S.A. AC32M nitrogen oxides analyzer) and are used as proxies for traffic emissions.

2.2.3 Radiocarbon analyses

All samples have been analyzed twice to increase the precision of $^{14}C/^{12}C$ and carbon mass data and to check for possible heterogeneity of individual filters. This represents a total of 124 measurements including the sampling blanks (4 field blanks for Chamonix and 12 for Passy). Blank sampling filters are treated as real samples (in the lab and in the field) with the exception that no actual sampling is carried out: they are used to ensure that no significant contamination occurs during the different steps of the sampling campaign (e.g. during storage or transport).

Punch surface required for radiocarbon analysis (i.e. punch of 1 cm^2 or 0.4 cm^2, depending on the carbon loading of the filter) was determined using the total carbon concentration previously determined by the EC/OC thermo-optical analysis at LGGE (Grenoble). In this study, the carbon quantity is also determined by the GIS before CO_2 injection into the ion source.

The mean carbon mass of the sampling blank filters determined by the GIS system is 1.75 µgC (SD = 1.22 µgC, N = 16). This contamination level agrees with the independent blank assessment described in Sect. 2.1.2. For real aerosol samples, the carbon mass and $^{14}C/^{12}C$ ratios are thus corrected in the same way as described previously.

The carbon content data measured by TOA in the LGGE (Grenoble) and by the GIS in the CEREGE (Aix-en-Provence) are compared in Fig. 5, exhibiting a very strong linear correlation for both sites (treated together). The slope is close to 1, with a very small intercept, suggesting there is no major difference between measurements obtained on different punch subsamples. This also demonstrates that sampling filters are loaded relatively homogenously.

3 Results and discussion

3.1 Composition of PM_{10}

For both sites, summer samples exhibit daily average PM_{10} concentrations up to 21 µg m^{-3} while winter PM_{10} concentrations range from 13 to 133 µg m^{-3}. Twelve days in Passy and three in Chamonix exceed 50 µg m^{-3} and correspond to winter smog episodes, above the public information threshold (see Table 3 and Table 4). On average, winter samples are composed of about 45% carbon (for both Passy and Chamonix), while summer samples in Passy comprise 25% carbon only. The carbon concentration in Passy is very high during the winter season (average of 23 µgC m^{-3}), particularly during December with a mean concentration of 40 µgC m^{-3}. It is much lower during July and August at about 3 µgC m^{-3}. The mean carbon concentration in Chamonix for December and January is about 18 µgC m^{-3}. Therefore, the December average carbon load in Passy is about twice that in Chamonix. Passy is a populated area, located in the lower part of the Arve Valley, with a valley constriction (steep slopes and reduced sun exposure) limiting atmospheric mixing in winter. High emissions and a strong temperature inversion layer persisting for several consecutive days lead to very high particle concentrations when compared to those in Chamonix.

These winter carbon concentrations are an order of magnitude higher than those determined in Gothenburg (Sweden) during February and March 2005 (3 µgC m^{-3}) (Szidat et al., 2009) or in Hachioji (Japan) during the 2003 and 2004 winter seasons (less than 3 µgC m^{-3}) (Uchida et al., 2010). Comparable concentrations were observed in Switzerland (Szidat et al., 2007), in Roverodo (about 16 µgC m^{-3}, January 2005) and Moleno (about 24 µgC m^{-3}, February 2005), places that are also typical Alpine valley sites similar to Passy and Chamonix.

The summer mean level of levoglucosan in Passy is close to 0.03 µg m^{-3} which is comparable to summer background concentrations determined by Puxbaum et al. (2007) for six background stations located on an east-west line from Hungary to the Azores. At our sites, winter levels are about 100 times greater than summer ones: in Chamonix, the average concentration is about 2.6 µg m^{-3} while in Passy about 3.4 µg m^{-3} (up to 8.5 µg m^{-3}). These levels are similar to those found in Launceston (Australia) during winter 2003 (Jordan et al., 2006a) but are generally higher than winter levels measured in various European cities (Herich et al., 2014).

Recent studies report that levoglucosan can be partially degraded by photo-oxidation (Hennigan et al., 2010; Kessler et al., 2010) for summer conditions, suggesting that this proxy is not as stable as previously thought. However, as winter temperatures are low (on average between 0 and -2.5 °C) and photo-oxidation is reduced by meteorological conditions (reduced daylight period, strong presence of smog and clouds) during this season, the levoglucosan level is expected to be particularly stable during winter. In addition, in our study, sampling was carried out close to the emissions sources, limiting the exposure time and thus any possible degradation even during summer time.

Levoglucosan emission rate depends on various factors, such as the combustion type and conditions (Engling et al., 2006; Schmidl et al., 2008; Lee et al., 2010). Wood type (softwoods and hardwoods) also has an influence on the emission factor of levoglucosan: as ambient measurements generally represents a mixture of different fuels and combustion conditions, the relation between levoglucosan and PM emissions can vary.

3.2 ^{14}C-based source apportionment

Carbon in atmospheric aerosols can originate from both fossil and contemporary sources. Carbon in particles from fossil fuel emissions is characterized by F^{14}C = 0, due to the radioactive decay (half-life of 5730 years), whereas F^{14}C ≈ 1 for carbon in particles coming from contemporary sources. In addition, the atmospheric thermonuclear bomb tests of the late 1950s and early 1960s increased the ^{14}C content of the atmosphere, leading to F^{14}C contemporary values greater than 1. In the northern hemisphere, the bomb spike reached F^{14}C values on the order of 1.8 in the early 1960s and it has decayed asymptotically since that time (Levin et al., 2010; Hua et al., 2013; Levin et al. 2013). From these studies, the atmospheric value for the year 2013-2014 can be estimated to $F^{14}C_{atmo}$ = 1.04. Hence, biogenic emissions from these years will present the same value ($F^{14}C_{atmo}$ = $F^{14}C_{bio}$ = 1.04).

3.2.1 Apportionment of the carbon pool with a simple hypothesis

In a first and preliminary approximation, we assume that the carbonaceous fraction is composed of both a fossil fraction, without ^{14}C and so linked to fossil fuels, and an isotopically homogenous non-fossil fraction. To determine this non-fossil fraction (f_{NF}), the measured F^{14}C has to be normalized by a non-fossil reference value ($f_{NF,ref}$, expressed in F^{14}C) as described by Eq. (6).

$$f_{NF} = \frac{F^{14}C}{f_{NF,ref}} \tag{6}$$

The high levels of levoglucosan obtained during winter illustrate the significance of biomass burning during this cold season at both sites while summer values suggest that very little biomass burning is recorded for this warm season. Biomass burning is mainly based on wood that grew over the past decades. This means that this carbon fraction integrates an average F^{14}C that is slightly higher than that of the atmosphere at the time of sampling. As per Szidat et al. (2006) and Lewis et al. (2004), we assume that wood used for biomass burning has an average $F^{14}C_{bb}$ = 1.10 ($f_{M,bb}$ = 1.09), which can be retrieved from the atmospheric ^{14}C record combined with a tree growth model.

For the summer season, it is considered that all non-fossil carbon originates from organic compounds naturally released by living plants (Guenther et al., 1995). No wild fire was recorded during the sampling period and the influence of the charcoal from barbecue cooking is neglected; levels of cholesterol, generally emitted by meat charbroiling (Schauer et al., 1999) remain very low, pointing that this cooking technique is not important here. Therefore, only the biogenic source of aerosols is considered, whose F^{14}C value should be close to the atmospheric value at the time of sampling ($F^{14}C_{bio}$ = 1.04).

Hence, for this first estimation of the non-fossil and fossil fractions, $f_{NF,ref}$ is estimated to be equal to 1.10 F^{14}C for the winter samples and to 1.04 F^{14}C for the summer ones.

The calculated non-fossil fraction (f_{NF}) for the winter samples (Fig. 6) exhibit high values, with mean values equal to 0.89 and 0.84 for Passy and Chamonix, respectively. Lower values observed at Passy in summer (mean f_{NF} = 0.75) indicate that the fossil component is more important in relative term to the total carbon content of aerosols, but that an important non-fossil fraction is still largely dominant.

The concentrations of non-fossil carbon (TC_{NF}) and fossil carbon (TC_F) can be calculated by multiplying the total carbon concentration TC by the non-fossil fraction (f_{NF}) and the fossil fraction (f_F) respectively.

While the mean TC is about 13 times larger in winter than summer, the fossil carbon concentration TC_F exhibit a smaller variation between seasons, as expected from similar traffics over the year. Nonetheless, the TC_F winter concentration is still about 3 times the summer one which may be related to the reduced atmospheric dynamics during winter, leading to trapping of particles by the inversion layers.

Schmidl et al. (2008) demonstrated that combustion of five biomass fuel types (spruce, larch, beech, oak and briquettes) at similar burning conditions leads to a wide range of total carbon to levoglucosan ratios from 4.3 to 17.2. In their study, the TC only originates from wood combustion and can thus be considered as completely non-fossil TC. The mean TC_{NF}/levoglucosan ratios equal 6.2 (SD = 0.4, N =28) for Passy and 6.0 (SD = 0.3, N = 13) for Chamonix. These ratios are within the range, but do not correspond to any particular wood type as presented by (Schmidl et al., 2008). However, the TC_{NF}/levoglucosan ratios for Chamonix and Passy are in good agreement to those obtained by Zotter et al. (2014) for several Swiss stations in the south Alps with ratios close to 6.2 ± 2.0, with the exception of Chiasso station (TC_{NF}/levo ratio about 9.1 ± 2.6).

The TC_{NF} values are plotted against levoglucosan in Fig. 7, and show a linear relation with high correlation coefficients for Chamonix (Pearson's R = 0.989) and Passy (Pearson's R = 0.995) samples. Moreover, the intercepts are not statistically different from zero showing that virtually all TC_{NF} during the winter originates from the burning of biomass and more specifically from wood combustion used for heating.

One interesting point with these excellent correlations is their stability for a large array of samples, which may include samples with various aging history and thus variable amount of secondary aerosols produced from VOCs emitted during biomass combustion. Nevertheless, the correlations are established between a primary tracer (levoglucosan) and a total carbon quantity that includes both primary and secondary carbonaceous aerosols. Therefore the excellent correlation implies either that the primary particles are dominant (in general for the total emission or because the secondary formation is slow in our conditions) or that the fraction of secondary particle is constant in relative terms (i.e. the correlation would remain even if secondary particles were dominant).

As a purely hypothetical case, let's assume that secondary organic aerosols (SOA) vary between 25% and 50% by OC mass of the primary organic aerosols (POA), according to VOC conversion kinetics (i.e. 25% in a recent air and 50% in an older one). The majority of carbonaceous aerosols would still be composed of primary aerosols, ranging from 80% to 67% of the total carbon, for the two end-members. However, because the dynamic range of total emissions is very large, this variability due to aerosol aging is difficult to detect on the TC_{NF} vs levoglucosan diagram (Fig. 7).

Keeping the same educated guess would imply that for a particular levoglucosan concentration value, one could observe a 20% range of TC_{NF} (i.e. 150/125 = 1.2). To illustrate this on Fig. 7, we show two extreme cases assuming only young air (i.e. SOA = 25 % of POA) or only older air (i.e. SOA = 50 % of POA). For the same value of levoglucosan, the TC_{NF} ratio between the two extremes should be 1.2, which can be approximated by decreasing or increasing the observed slope by about 10% (dotted lines in Fig. 7) around the observed correlation assumed to be centered between the two end-members. Even if the observed correlation in Fig. 7 is strong, it is clear that its scatter is not completely negligible, but is within the variation between the two hypothetical extremes (see for examples the TC_{NF} values corresponding to about 6 µg m^{-3} of levoglucosan). These observations and speculations would certainly justify specific studies on secondary aerosol formation processes in the atmospheric conditions of the Arve valley.

During summer, domestic heating emissions are presumed to be weak, as confirmed by really low levoglucosan concentrations. Levoglucosan and TC_{NF} concentrations show no correlation for summer samples (represented by blue dots in Fig. 7). As mentioned above, TC_{NF} still represents 75% of the total carbon on average in summer. It has already been demonstrated that the modern sources of carbon are dominant over the fossil fuel ones in atmospheric PM of many sites, even in a large city like Marseille, France (El Haddad et al., 2011). It is also the case in these more rural environments. These TC_{NF} levels are about four times higher than expected by the regression model determined for the winter samples, if they were due to biomass burning. These results indicate that the main non-fossil sources differ between seasons. For the winter season, TC_{NF} is directly related to biomass burning, whereas during summer these sources are most probably biogenic emissions.

To attribute the fossil fraction of the carbonaceous particles, the concentrations of fossil carbon (TC_F) are plotted against NO_X concentration (Fig. 8), which is considered as a vehicle emission proxy. Linear correlations are highly statistically significant for all three different datasets. All origin intercepts are equivalent or close to zero. For winter data sets, the slope obtained for the French data sets are roughly equivalent to those given by Zotter et al. (2014) for the EC_F vs. NO_X correlations in many Swiss sites (no correlations were observed with OC_F in this last study). However, in our study, the slopes for Passy and Chamonix are clearly different, with that in Passy being 50% higher. The reason for such a difference is currently unknown, but may be related to the vehicle fleet influencing the two sites: while the site in Chamonix is an urban traffic site with only passenger vehicles, the site in Passy is an urban background site 1 km away from the highway to Italy supporting a large international truck traffic. Also, the impact of some industrial emissions in Passy remains to be investigated.

The slope obtained for the summer samples (only in Passy) is larger than that obtained for winter, which may suggest different vehicular emissions in summer than in winter or an extensive degradation of NO_X during summer. Another hypothesis is that secondary formation of OC from vehicular gaseous emissions may well be greater in summer than in winter.

3.2.2 Apportionment with biogenic fraction variations

The calculations above only constitute a first approximation which takes into account a single non-fossil source to define $f_{NF,ref}$. So far, we considered the non-fossil source to be purely biogenic during summer and to originate exclusively from biomass burning only during winter. However, the non-fossil carbon is made up of these two different fractions which differ slightly in their $^{14}C/^{12}C$ ratios and both have to be acknowledged in the definition of $f_{NF,ref}$.

Zhang et al. (2012) assumed a biogenic fraction (p_{bio}) constant throughout the year, implying that its origin does not vary with the season. More recently, Zotter et al. (2014) applied a variability with the seasons: the biogenic fraction is set at 0.4 during summer and 0.2 during winter, since no large contributions from biogenic sources are expected during the cold season. With these two assumptions, the maximum $F^{14}C$ value in the absence of a fossil component is given by the following mass balance equation Eq. (7) (Szidat et al., 2006; Zhang et al., 2012; Zotter et al., 2014):

$$f_{NF\ ref} = p_{bio} \times F^{14}C_{bio} + (1 - p_{bio}) \times\ F^{14}C_{bb} \tag{7}$$

where $F^{14}C_{\ bio}$ and $F^{14}C_{\ bb}$ correspond to the $F^{14}C$ values of the biogenic (1.04) and the biomass burning components (1.10), respectively. Similarly, p_{bio} corresponds to the biogenic fraction in the total non-fossil carbon, whereas the biomass burning fraction is simply ($1-p_{bio}$). Figure 6 shows the time series of the f_{NF} values calculated by using both the simple and sophisticated models for both sites. In all cases, it must be noted that introducing various values of p_{bio} has a minor impact on $f_{NF,ref.}$ Indeed, a decrease of p_{bio} from 1 to 0 would change $f_{NF,ref}$ by 6%. In the same way, the regression parameters for the TC_{NF} vs. levoglucosan correlations are listed in Table 5 for the different values of $f_{NF,ref}$ (*i.e.* with p_{bio} = 1, 0.4, 0.2 and 0). It can be seen that the small variation of $f_{NF,ref}$ has a negligible impact on the linear regression parameters. All approaches confirm the dominance of the biomass burning component during winter as illustrated in Fig. 6.

Table 5 also provides all parameters for the TC_F vs NO_X linear fits. Again, correlation coefficients are significant for all values of p_{bio} (1, 0.4, 0.2 and 0) confirming that introducing the hypotheses for this second model is not leading to changes in the source partitioning.

3.2.3 Apportionment for summer samples: independent determination of the non-fossil fraction

One inherent problem with the previous model is that it relies on a priori assumptions about the sources of the non-fossil fraction. In addition, it assumes that the biomass burning and biogenic concentrations (TC_{bb} and TC_{bio}) are proportional to TC_{NF} which also implies a linear correlation between the two fractions, i.e. $TC_{bb} = [(1-p_{bio})/p_{bio}]xTC_{bio}$. Indeed, one could well imagine a variable emission of biomass burning superimposed on a rather constant emission of biogenic particles, or even a more complex situation as the two sources have different and rather independent origins.

In Sect. 3.2.1, the nearly exclusive contribution of biomass burning to the non-fossil fraction during winter has been demonstrated by the strong linear correlation between levoglucosan and TC_{NF} (Fig. 7 and Table 5) and by intercepts nearly equal to zero (i.e. $TC_{NF} \approx TC_{bb}$ during winter). For summer samples, the insert in Fig. 7 shows that the TC_{bb} expected by the linear models is lower than the measured TC_{NF} suggesting another source of non-fossil carbon.

As an alternative model, we tentatively propose that the part of TC_{NF} due to biomass burning (TC_{bb}) in a particular sample could be calculated from its levoglucosan concentration by using its linear correlation to TC_{NF} observed in winter (i.e. TC_{bb} = a x [levoglucosan], a being the slope of the linear relationship shown in Fig. 7).

Total carbon TC is composed of both fossil TC_F and non-fossil fraction TC_{NF}. The latter can be sub-divided in parts corresponding to the considered sources, i.e. biomass burning and biogenic emissions (TC_{bb} and TC_{bio} respectively)

$$TC = TC_{NF} + TC_F = TC_{bb} + TC_{bio} + TC_F \quad (8)$$

This leads to the following ^{14}C mass balance:

$$TC \times F^{14}C_S = TC_{bb} \times F^{14}C_{bb} + TC_{bio} \times F^{14}C_{bio} + TC_F \times F^{14}C_F = TC_{bb} \times F^{14}C_{bb} + TC_{bio} \times F^{14}C_{bio} \quad (9)$$

With $F^{14}C_S$ the measured $^{14}C/^{12}C$ ratio of the sample, $F^{14}C_{bb}$ = 1.10, $F^{14}C_{bio}$ = 1.04 and $F^{14}C_F$ = 0 as previously discussed in Sect. 3.2.1. TC is the total carbon of the sample [µgC m^{-3}], TC_{bb} the carbon originating from biomass burning, TC_{bio} the carbon from biogenic emissions and finally TC_F from fossil sources.

It is thus possible to calculate the biogenic fraction and the fossil fraction by combining the ^{14}C mass balance in Eq. (10) and the total carbon mass balance in Eq. (11):

$$TC_{bio} = \frac{F^{14}C_S \times TC - TC_{bb} \times F^{14}C_{bb}}{F^{14}C_{bio}} \quad (10)$$

$$TC_F = TC - TC_{bb} - TC_{bio} \quad (11)$$

The results for summer samples are provided in Table 6. It should be stressed that this model relies on the hypothesis that levoglucosan does not suffer from a large differential degradation between summer and winter, which may be valid to a first order as PM sampling have been carried out close to the emissions sources. The contribution of fossil carbon to TC is estimated to be about 25 %, corresponding to very low fossil carbon concentration i.e. 0.80 µgC m^{-3}. By contrast, the results point to a major contribution of about 87 % and up to 93 % of biogenic emissions to the non-fossil fraction (i.e. p_{bio} is about 0.9).

The biogenic carbon concentrations (TC_{bio}) can be compared to the concentrations of polyols as these sugar-alcohols are known to be tracers for primary biogenic aerosol particles (Yttri et al., 2007). As shown in Fig. 9, there is no simple relationship between TC_{bio} and polyols for the summer samples, indicating that despite its potential to be a large contributor to PM_{10} in some environments (Waked et al, 2014), this source may not be dominant in the modern fraction of carbon in summer in the Arve Valley.

TC_{bio} includes both primary and secondary organic aerosols, which result from the oxidation of biogenic volatile organic carbon compounds (BVOCs). It is known that BVOCs emissions generally follow the temperature (Leaitch et al., 2011). Indeed, Fig. 10 shows that TC_{bio} increases with the mean temperature during the warmest part of the day (from 10 am to 6 pm) defining a significant linear correlation (Pearson's coefficient of 0.65 with a slope of 0.27 ± 0.05 and y-intercept of -3.41 ± 1.06). Given the physiological effect of temperature, it is logical to expect that emissions are negligible at the low temperature, which can be approximated by an exponential law given in Eq. (12) as in Leaitch et al. (2011).

$$TC_{bio} = \alpha \times \exp(\beta \times T) \quad (12)$$

Where T is expressed in degrees Celsius, α is a constant, which could be assimilated to a base capacity and β is an empirical constant. By studying the linear correlation between $\ln(TC_{bio})$ and temperature, it is possible to calculate α = 0.12 ± 0.02 and β = 0.16 (+0.09 /– 0.06), with a Pearson's coefficient of 0.72. The correlation coefficient is thus slightly higher for the exponential law than for the linear model. In any case, the fact that TC_{bio} depends on temperature suggests that this fraction is mainly composed of secondary organic aerosol.

Conclusion

Quantifying the relative contribution of fossil and non-fossil sources of carbonaceous aerosols is important in order to better understand the sources of atmospheric particles and to attribute them to natural and anthropogenic processes. For example, both biomass burning for domestic heating and road traffic emissions are known to contribute to PM pollution in many urban areas, notably in the Arve Valley (French Alps) which is the focus of the present study.

Radiocarbon (^{14}C) analysis is the best way to distinguish fossil fuel combustion products from other carbon sources such as biomass burning and biogenic emissions. We show here that ^{14}C is efficiently measured in aerosol samples with the AixMICADAS spectrometer by using an elemental analyzer (EA) coupled to its CO_2 gas ion source, which can handle small samples (10-100 µgC). This direct coupling avoids the production of solid graphite targets, the usual bottleneck in traditional radiocarbon measurement by accelerator mass spectrometry. The present work leads to the following conclusions:

_ Contamination of the measurement procedure is mainly linked to the silver boats in which the filter samples are wrapped prior to combustion in the EA. This contamination has been quantified and shown to be fairly constant, which enables rectification of the measurements of aerosol samples.

_ The precision and accuracy of ^{14}C measurements in aerosols are validated over the full range of expected fossil and non-fossil carbon values by using various standards and synthetic mixtures.

_ Carbon concentrations of aerosols determined by thermal-optical analysis (LGGE in Grenoble) and GIS quantification (CEREGE in Aix-en-Provence) in samples from Passy and Chamonix are in excellent agreement and indicate large concentrations up to 50 µgC m^{-3} during winters.

_ Mean winter carbon concentrations are higher than those reported for several urban sites but are in the range of those measured in other alpine sites.

_ Levoglucosan content is used as a biomass burning proxy, indicating very high levels during winter with values up to 8 µg m^{-3} in Passy, thus higher than those generally observed in several European cities.

_ Based on ^{14}C measurements, the fractions of non-fossil carbon determined in winter (0.89 for Passy and 0.84 for Chamonix) are higher than the non-fossil fraction obtained for Passy during summer (0.75). However, the non-fossil fraction remains dominant during summer with a fossil contribution of about 25%, probably from road traffic.

_ Non-fossil carbon concentration (TC_{NF}) is strongly correlated with levoglucosan concentration for winter samples (Passy and Chamonix). The linear regression intercepts are close to zero suggesting that almost all of the non-fossil carbon originates from biomass burning and more specifically from wood combustion used for heating during the winter.

_ Fossil carbon concentrations exhibit a strong correlation with NO_X concentrations, suggesting that the source of fossil carbon is directly linked to traffic emissions.

_ Summer samples exhibit an important relative contribution of non-fossil sources (75 %). A dual approach based on ^{14}C and levoglucosan enables the calculation of a first estimation of the biogenic and biomass burning fractions in the non-fossil carbon. The samples from Passy allow to test this new model, suggesting that for this site the biogenic emissions are the most important contributor to the non-fossil fraction during summer.

_ The lack of correlation between polyols (tracers of biogenic activity in soil) and the biogenic fraction suggest that TC_{bio} could be composed of secondary organic aerosols resulting from the oxidation of biogenic VOC which is also suggests by the correlation between TC_{bio} and temperature.

Overall, combining radiocarbon and levoglucosan measurements strengthens findings concerning the dominant contribution of winter biomass burning to aerosols in the Arve Valley. In addition to first order agreement, both tracers are complementary: levoglucosan enables to identify the source while ^{14}C allows to precisely quantify the fossil and non-fossil fractions.

We show that this dual approach may also serve to go further in quantifying these additional carbon sources. Combining ^{14}C and levoglucosan measurements allows reconstructing other contributions such as biogenic aerosols fluxes. As an example, our new model is applied to summer samples from Passy leading to reasonable evaluations of biogenic particle fluxes. These aerosols are probably linked to oxidation of volatile organic compounds (VOCs) as suggested by a significant correlation of fluxes with temperature.

Following Zhang et al. (2012) ongoing research at CEREGE into ^{14}C measurements of separated elemental carbon and organic carbon fractions of aerosol should provide more precise source apportionment in the future.

Acknowledgements

AixMICADAS was acquired and is operated in the framework of the EQUIPEX project ASTER-CEREGE (PI E. Bard) with additional matching funds from the Collège de France, which also supports the salaries of the authors from CEREGE. We thank Sönke Szidat for advice on reporting ^{14}C results in aerosols.

References

Aymoz, G., Jaffrezo, J. L., Chapuis, D., Cozic, J. and Maenhaut, W.: Seasonal variation of PM10 main constituents in two valleys of the French Alps. I: EC/OC fractions, Atmos Chem Phys, 7(3), 661–675, doi:10.5194/acp-7-661-2007, 2007.

Bard, E., Tuna, T., Fagault, Y., Bonvalot, L., Wacker, L., Fahrni, S. and Synal, H.-A.: AixMICADAS, the accelerator mass spectrometer dedicated to 14C recently installed in Aix-en-Provence, France, Nucl. Instrum. Methods Phys. Res. Sect. B Beam Interact. Mater. At., 361, 80–86, doi:10.1016/j.nimb.2015.01.075, 2015.

Bauer, H., Claeys, M., Vermeylen, R., Schueller, E., Weinke, G., Berger, A. and Puxbaum, H.: Arabitol and mannitol as tracers for the quantification of airborne fungal spores, Atmos. Environ., 42(3), 588–593, doi:10.1016/j.atmosenv.2007.10.013, 2008.

Birch, M. E. and Cary, R. A.: Elemental Carbon-Based Method for Monitoring Occupational Exposures to Particulate Diesel Exhaust, Aerosol Sci. Technol., 25(3), 221–241, doi:10.1080/02786829608965393, 1996.

Bond, T. C., Doherty, S. J., Fahey, D. W., Forster, P. M., Berntsen, T., DeAngelo, B. J., Flanner, M. G., Ghan, S., Kärcher, B., Koch, D., Kinne, S., Kondo, Y., Quinn, P. K., Sarofim, M. C., Schultz, M. G., Schulz, M., Venkataraman, C., Zhang, H., Zhang, S., Bellouin, N., Guttikunda, S. K., Hopke, P. K., Jacobson, M. Z., Kaiser, J. W., Klimont, Z., Lohmann, U., Schwarz, J. P., Shindell, D., Storelvmo, T., Warren, S. G. and Zender, C. S.: Bounding the role of black carbon in the climate system: A scientific assessment, J. Geophys. Res. Atmospheres, 118(11), 5380–5552, doi:10.1002/jgrd.50171, 2013.

Caseiro, A., Bauer, H., Schmidl, C., Pio, C. A. and Puxbaum, H.: Wood burning impact on PM10 in three Austrian regions, Atmos. Environ., 43(13), 2186–2195, doi:10.1016/j.atmosenv.2009.01.012, 2009.

Cavalli, F., Viana, M., Yttri, K. E., Genberg, J. and Putaud, J.-P.: Toward a standardised thermal-optical protocol for measuring atmospheric organic and elemental carbon: the EUSAAR protocol, Atmos Meas Tech, 3(1), 79–89, doi:10.5194/amt-3-79-2010, 2010.

Cavanagh, R. R. and Watters, R. L.: National Institute of Standards & Technology. Report of Investigation Reference Material 8785 Air Particulate Matter on Filter Media (A Fine Fraction of SRM 1649a Urban Dust on Quartz-Fiber Filter), 2005.

Chevrier, F., Brulfert, G., Mocnik, G., Marchand, N., Jaffrezo, J.-L. and Besombes, J.-L.: DECOMBIO - Contribution de la combustion de la biomasse aux PM10 en vallée de l'Arve : mise en place et qualification d'un dispositif de s, Poll. Atmos, In Press., Pollut. Atmos. Press, 2016.

Chung, S. H. and Seinfeld, J. H.: Global distribution and climate forcing of carbonaceous aerosols, J. Geophys. Res. Atmospheres, 107(D19), 4407, doi:10.1029/2001JD001397, 2002.

Currie, L. A. and Kessler, J. D.: On the isolation of elemental carbon (EC) for micro-molar 14C accelerator mass spectrometry: development of a hybrid reference material for 14C-EC accuracy assurance, and a critical evaluation of the thermal optical kinetic (TOK) EC isolation procedure, Atmos Chem Phys, 5, 2833–2845, 2005.

Currie, L. A., Klouda, G. A. and Voorhees, K. J.: Atmospheric carbon: The importance of accelerator mass spectrometry, Nucl. Instrum. Methods Phys. Res. Sect. B Beam Interact. Mater. At., 5(2), 371–379, doi:10.1016/0168-583X(84)90544-5, 1984.

Currie, L. A., Stafford, T. W., Sheffield, A. E., Klouda, G. A., Wise, S. A., Fletcher, R. A., Donahue, D. J., Jull, A. J. T. and Linick, T. W.: Microchemical and molecular dating., Radiocarbon, 31(3), 448–463, doi:10.2458/azu_js_rc.31.1171, 1989.

Currie, L. A., Benner Jr., B. A., Kessler, J. D., Klinedinst, D. B., Klouda, G. A. ., Marolf, J. V., Slater, J. F., Wise, S. A., Cachier, H., Cary, R., Chow, J. C., Watson, J., Druffel, E. R. M., Masiello, C. A., Eglinton, T. I., Pearson, A., Reddy, C. M., Gustafsson, O., Hartmann, P. C., Quinn, J. G., Hedges, J. I., Prentice, K. M., Kirchstetter, T. W., Novakov, T., Puxbaum, H. and Schmid, H.: A Critical Evaluation of Interlaboratory Data on Total, Elemental, and Isotopic Carbon in the Carbonaceous Particle Reference Material, NIST SRM 1649a, J. Res. Natl. Inst. Stand. Technol., 107(3), 279–298, 2002.

El Haddad, I., Marchand, N., Wortham, H., Piot, C., Besombes, J.-L., Cozic, J., Chauvel, C., Armengaud, A., Robin, D. and Jaffrezo, J.-L.: Primary sources of PM2.5 organic aerosol in an industrial Mediterranean city, Marseille, Atmos Chem Phys, 11(5), 2039–2058, doi:10.5194/acp-11-2039-2011, 2011.

Engling, G., Carrico, C. M., Kreidenweis, S. M., Collett Jr., J. L., Day, D. E., Malm, W. C., Lincoln, E., Min Hao, W., Iinuma, Y. and Herrmann, H.: Determination of levoglucosan in biomass combustion aerosol by high-performance anion-exchange chromatography with pulsed amperometric detection, Atmos. Environ., 40, Supplement 2, 299–311, doi:10.1016/j.atmosenv.2005.12.069, 2006.

Eriksson Stenström, K., Skog, G., Georgiadou, E., Genberg, J. and Johansson, A.: A guide to radiocarbon units and calculations, Lund University., 2011.

Fahrni, S. M., Wacker, L., Synal, H.-A. and Szidat, S.: Improving a gas ion source for 14C AMS, Nucl. Instrum. Methods Phys. Res. Sect. B Beam Interact. Mater. At., 294, 320–327, doi:10.1016/j.nimb.2012.03.037, 2013.

Favez, O., El Haddad, I., Piot, C., Boréave, A., Abidi, E., Marchand, N., Jaffrezo, J.-L., Besombes, J.-L., Personnaz, M.-B., Sciare, J., Wortham, H., George, C. and D'Anna, B.: Inter-comparison of source apportionment models for the estimation of wood burning aerosols during wintertime in an Alpine city (Grenoble, France), Atmos Chem Phys, 10(12), 5295–5314, doi:10.5194/acp-10-5295-2010, 2010.

Genberg, J., Stenström, K., Elfman, M. and Olsson, M.: Development of graphitization of μ-sized samples at Lund University, Radiocarbon, 52(2–3), 1270–1276, 2010.

Genberg, J., Perron, N., Olsson, M. and Stenstrom, K.: Sealed glass tube combustion of μg-sized aerosol samples, Radiocarbon, 55(2–3), 617–623, 2013.

Guenther, A., Hewitt, C. N., Erickson, D., Fall, R., Geron, C., Graedel, T., Harley, P., Klinger, L., Lerdau, M., Mckay, W. A., Pierce, T., Scholes, B., Steinbrecher, R., Tallamraju, R., Taylor, J. and Zimmerman, P.: A global model of natural volatile organic compound emissions, J. Geophys. Res. Atmospheres, 100(D5), 8873–8892, doi:10.1029/94JD02950, 1995.

Gustafsson, Ö., Kruså, M., Zencak, Z., Sheesley, R. J., Granat, L., Engström, E., Praveen, P. S., Rao, P. S. P., Leck, C. and Rodhe, H.: Brown Clouds over South Asia: Biomass or Fossil Fuel Combustion?, Science, 323(5913), 495–498, doi:10.1126/science.1164857, 2009.

Heal, M. R., Naysmith, P., Cook, G. T., Xu, S., Duran, T. R. and Harrison, R. M.: Application of 14C analyses to source apportionment of carbonaceous PM2.5 in the UK, Atmos. Environ., 45(14), 2341–2348, doi:10.1016/j.atmosenv.2011.02.029, 2011.

Hennigan, C. J., Sullivan, A. P., Collett, J. L. and Robinson, A. L.: Levoglucosan stability in biomass burning particles exposed to hydroxyl radicals, Geophys. Res. Lett., 37(9), L09806, doi:10.1029/2010GL043088, 2010.

Herich, H., Gianini, M. F. D., Piot, C., Močnik, G., Jaffrezo, J.-L., Besombes, J.-L., Prévôt, A. S. H. and Hueglin, C.: Overview of the impact of wood burning emissions on carbonaceous aerosols and PM in large parts of the Alpine region, Atmos. Environ., 89, 64–75, doi:10.1016/j.atmosenv.2014.02.008, 2014.

Hua, Q., Barbetti, M. and Rakowski, A. Z.: Atmospheric Radiocarbon for the Period 1950–2010, Radiocarbon, 55(4), 2059–2072, doi:10.2458/azu_js_rc.v55i2.16177, 2013.

Jacobson, M. C., Hansson, H.-C., Noone, K. J. and Charlson, R. J.: Organic atmospheric aerosols: Review and state of the science, Rev. Geophys., 38(2), 267–294, doi:10.1029/1998RG000045, 2000.

Jerrett, M., Burnett, R. T., Ma, R., Pope, C. A., Krewski, D., Newbold, K. B., Thurston, G., Shi, Y., Finkelstein, N., Calle, E. E. and Thun, M. J.: Spatial analysis of air pollution and mortality in Los Angeles, Epidemiol. Camb. Mass, 16(6), 727–736, 2005.

Jordan, T. B., Seen, A. J. and Jacobsen, G. E.: Levoglucosan as an atmospheric tracer for woodsmoke, Atmos. Environ., 40(27), 5316–5321, doi:10.1016/j.atmosenv.2006.03.023, 2006a.

Jordan, T. B., Seen, A. J., Jacobsen, G. E. and Gras, J. L.: Radiocarbon determination of woodsmoke contribution to air particulate matter in Launceston, Tasmania, Atmos. Environ., 40(14), 2575–2582, doi:10.1016/j.atmosenv.2005.12.024, 2006b.

Kennedy, I. M.: The health effects of combustion-generated aerosols, Proc. Combust. Inst., 31(2), 2757–2770, doi:10.1016/j.proci.2006.08.116, 2007.

Kessler, S. H., Smith, J. D., Che, D. L., Worsnop, D. R., Wilson, K. R. and Kroll, J. H.: Chemical Sinks of Organic Aerosol: Kinetics and Products of the Heterogeneous Oxidation of Erythritol and Levoglucosan, Environ. Sci. Technol., 44(18), 7005–7010, doi:10.1021/es101465m, 2010.

Klouda, G. A., Filliben, J. J., Parish, H. J., Chow, J. C., Watson, J. G. and Cary, R. A.: Reference Material 8785: Air Particulate Matter on Filter Media, Aerosol Sci. Technol., 39(2), 173–183, doi:10.1080/027868290916453, 2005.

Leaitch, W. R., Macdonald, A. M., Brickell, P. C., Liggio, J., Sjostedt, S. J., Vlasenko, A., Bottenheim, J. W., Huang, L., Li, S.-M., Liu, P. S. K., Toom-Sauntry, D., Hayden, K. A., Sharma, S., Shantz, N. C., Wiebe, H. A., Zhang, W., Abbatt, J. P. D., Slowik, J. G., Chang, R. Y.-W., Russell, L. M., Schwartz, R. E., Takahama, S., Jayne, J. T. and Ng, N. L.: Temperature response of the submicron organic aerosol from temperate forests, Atmos. Environ., 45(37), 6696–6704, doi:10.1016/j.atmosenv.2011.08.047, 2011.

Lee, T., Sullivan, A. P., Mack, L., Jimenez, J. L., Kreidenweis, S. M., Onasch, T. B., Worsnop, D. R., Malm, W., Wold, C. E., Hao, W. M. and Jr, J. L. C.: Chemical Smoke Marker Emissions During Flaming and Smoldering Phases of Laboratory Open Burning of Wildland Fuels, Aerosol Sci. Technol., 44(9), i–v, doi:10.1080/02786826.2010.499884, 2010.

Lelieveld, J., Evans, J. S., Fnais, M., Giannadaki, D. and Pozzer, A.: The contribution of outdoor air pollution sources to premature mortality on a global scale, Nature, 525(7569), 367–371, doi:10.1038/nature15371, 2015.

Levin, I. and Kromer, B.: The tropospheric (super 14) CO (sub 2) level in mid-latitudes of the Northern Hemisphere (1959-2003)., Radiocarbon, 46(3), 1261–1272, doi:10.2458/azu_js_rc.46.4181, 2004.

Levin, I., Naegler, T., Kromer, B., Diehl, M., Francey, R. J., Gomez-Pelaez, A. J., Steele, L. P., Wagenbach, D., Weller, R. and Worthy, D. E.: Observations and modelling of the global distribution and long-term trend of atmospheric 14 CO 2, Tellus B, 62(1), 26–46, doi:10.1111/j.1600-0889.2009.00446.x, 2010.

Levin, I., Kromer, B. and Hammer, S.: Atmospheric Δ 14 CO 2 trend in Western European background air from 2000 to 2012, Tellus B, 65(0) [online] Available from: http://www.tellusb.net/index.php/tellusb/article/view/20092 (Accessed 5 May 2015), 2013.

Lewis, C. W., Klouda, G. A. and Ellenson, W. D.: Radiocarbon measurement of the biogenic contribution to summertime PM-2.5 ambient aerosol in Nashville, TN, Atmos. Environ., 38(35), 6053–6061, doi:10.1016/j.atmosenv.2004.06.011, 2004.

Liu, D., Li, J., Zhang, Y., Xu, Y., Liu, X., Ding, P., Shen, C., Chen, Y., Tian, C. and Zhang, G.: The Use of Levoglucosan and Radiocarbon for Source Apportionment of PM2.5 Carbonaceous Aerosols at a Background Site in East China, Environ. Sci. Technol., 47(18), 10454–10461, doi:10.1021/es401250k, 2013.

Marchand, N., Besombes, J. L., Chevron, N., Masclet, P., Aymoz, G. and Jaffrezo, J. L.: Polycyclic aromatic hydrocarbons (PAHs) in the atmospheres of two French alpine valleys: sources and temporal patterns, Atmos Chem Phys, 4(5), 1167–1181, doi:10.5194/acp-4-1167-2004, 2004.

Penner, J. E., Chuang, C. C. and Grant, K.: Climate forcing by carbonaceous and sulfate aerosols, Clim. Dyn., 14(12), 839–851, doi:10.1007/s003820050259, 1998.

Pope, C. A. I. and Dockery, D. W.: Health Effects of Fine Particulate Air Pollution: Lines that Connect, J. Air Waste Manag. Assoc., 56(6), 709–742, doi:10.1080/10473289.2006.10464485, 2006.

Pöschl, U.: Atmospheric Aerosols: Composition, Transformation, Climate and Health Effects, Angew. Chem. Int. Ed., 44(46), 7520–7540, doi:10.1002/anie.200501122, 2005.

Putaud, J.-P., Raes, F., Van Dingenen, R., Brüggemann, E., Facchini, M.-C., Decesari, S., Fuzzi, S., Gehrig, R., Hüglin, C., Laj, P., Lorbeer, G., Maenhaut, W., Mihalopoulos, N., Müller, K., Querol, X., Rodriguez, S., Schneider, J., Spindler, G., Brink, H. ten, Tørseth, K. and Wiedensohler, A.: A European aerosol phenomenology—2: chemical characteristics of particulate matter at kerbside, urban, rural and background sites in Europe, Atmos. Environ., 38(16), 2579–2595, doi:10.1016/j.atmosenv.2004.01.041, 2004.

Putaud, J.-P., Van Dingenen, R., Alastuey, A., Bauer, H., Birmili, W., Cyrys, J., Flentje, H., Fuzzi, S., Gehrig, R., Hansson, H. C., Harrison, R. M., Herrmann, H., Hitzenberger, R., Hüglin, C., Jones, A. M., Kasper-Giebl, A., Kiss, G., Kousa, A., Kuhlbusch, T. A. J., Löschau, G., Maenhaut, W., Molnar, A., Moreno, T., Pekkanen, J., Perrino, C., Pitz, M., Puxbaum, H., Querol, X., Rodriguez, S., Salma, I., Schwarz, J., Smolik, J., Schneider, J., Spindler, G., ten Brink, H., Tursic, J., Viana, M., Wiedensohler, A. and Raes, F.: A European aerosol phenomenology – 3: Physical and chemical characteristics of particulate matter from 60 rural, urban, and kerbside sites across Europe, Atmos. Environ., 44(10), 1308–1320, doi:10.1016/j.atmosenv.2009.12.011, 2010.

Puxbaum, H., Caseiro, A., Sánchez-Ochoa, A., Kasper-Giebl, A., Claeys, M., Gelencsér, A., Legrand, M., Preunkert, S. and Pio, C.: Levoglucosan levels at background sites in Europe for assessing the impact of biomass combustion on the European aerosol background, J. Geophys. Res. Atmospheres, 112(D23), D23S05, doi:10.1029/2006JD008114, 2007.

Ramanathan, V., Crutzen, P. J., Kiehl, J. T. and Rosenfeld, D.: Aerosols, Climate, and the Hydrological Cycle, Science, 294(5549), 2119–2124, doi:10.1126/science.1064034, 2001a.

Ramanathan, V., Crutzen, P. J., Lelieveld, J., Mitra, A. P., Althausen, D., Anderson, J., Andreae, M. O., Cantrell, W., Cass, G. R., Chung, C. E., Clarke, A. D., Coakley, J. A., Collins, W. D., Conant, W. C., Dulac, F., Heintzenberg, J., Heymsfield, A. J., Holben, B., Howell, S., Hudson, J., Jayaraman, A., Kiehl, J. T., Krishnamurti, T. N., Lubin, D., McFarquhar, G., Novakov, T., Ogren, P. K., Podgorny, I. A., Prather, K., Priestley, K., Prospero, J. M., Quinn, P. K., Rajeev, K., Rasch, P., Rupert, S., Sadourny, R., Satheesh, S. K., Shaw, G. E., Sheridan, P. and Valero, F. P. J.: Indian Ocean Experiment: An integrated analysis of the climate forcing and effects of the great Indo-Asian haze, J. Geophys. Res., 106(D22), 28371–28398, 2001b.

Reimer, P. J., Brown, T. A. and Reimer, R. W.: Discussion: Reporting and Calibration of Post-Bomb 14C Data, Radiocarbon, 46(3), 1299–1304, doi:10.2458/azu_js_rc.46.4183, 2004.

Ruff, M., Szidat, S., Gäggeler, H. W., Suter, M., Synal, H.-A. and Wacker, L.: Gaseous radiocarbon measurements of small samples, Nucl. Instrum. Methods Phys. Res. Sect. B Beam Interact. Mater. At., 268(7–8), 790–794, doi:10.1016/j.nimb.2009.10.032, 2010a.

Ruff, M., Fahrni, S., Gäggeler, H. W., Hajdas, I., Suter, M., Synal, H.-A., Szidat, S. and Wacker, L.: On-line radiocarbon measurements of small samples using elemental analyser and MICADAS gas ion source, Radiocarbon, 52(4), 1645–1656, 2010b.

Salazar, G., Zhang, Y. L., Agrios, K. and Szidat, S.: Development of a method for fast and automatic radiocarbon measurement of aerosol samples by online coupling of an elemental analyzer with a MICADAS AMS, Nucl. Instrum. Methods Phys. Res. Sect. B Beam Interact. Mater. At., 361, 163–167, doi:10.1016/j.nimb.2015.03.051, 2015.

Schauer, J. J., Kleeman, M. J., Cass, G. R. and Simoneit, B. R. T.: Measurement of Emissions from Air Pollution Sources. 3. C1−C29 Organic Compounds from Meat Charbroiling, Environ. Sci. Technol., 33(10), 1566-1577, doi: 10.1021/es980076j, 1999.

Schauer, J. J., Kleeman, M. J., Cass, G. R. and Simoneit, B. R. T.: Measurement of Emissions from Air Pollution Sources. 3. C1−C29 Organic Compounds from Fireplace Combustion of Wood, Environ. Sci. Technol., 35(9), 1716–1728, doi:10.1021/es001331e, 2001.

Schmidl, C., Marr, I. L., Caseiro, A., Kotianová, P., Berner, A., Bauer, H., Kasper-Giebl, A. and Puxbaum, H.: Chemical characterisation of fine particle emissions from wood stove combustion of common woods growing in mid-European Alpine regions, Atmos. Environ., 42(1), 126–141, doi:10.1016/j.atmosenv.2007.09.028, 2008.

Simoneit, B. R. T., Schauer, J. J., Nolte, C. G., Oros, D. R., Elias, V. O., Fraser, M. P., Rogge, W. F. and Cass, G. R.: Levoglucosan, a tracer for cellulose in biomass burning and atmospheric particles, Atmos. Environ., 33(2), 173–182, doi:10.1016/S1352-2310(98)00145-9, 1999.

Stuiver, M.: International agreements and the use of the new oxalic acid standard, Radiocarbon, 25(2), 793–795, 1983.

Synal, H.-A., Stocker, M. and Suter, M.: MICADAS: A new compact radiocarbon AMS system, Nucl. Instrum. Methods Phys. Res. Sect. B Beam Interact. Mater. At., 259(1), 7–13, doi:10.1016/j.nimb.2007.01.138, 2007.

Szidat, S., Jenk, T. M., Gäggeler, H. W., Synal, H.-A., Hajdas, I., Bonani, G. and Saurer, M.: THEODORE, a two-step heating system for the EC/OC determination of radiocarbon (14C) in the environment, Nucl. Instrum. Methods Phys. Res. Sect. B Beam Interact. Mater. At., 223–224, 829–836, doi:10.1016/j.nimb.2004.04.153, 2004.

Szidat, S., Jenk, T. M., Synal, H.-A., Kalberer, M., Wacker, L., Hajdas, I., Kasper-Giebl, A. and Baltensperger, U.: Contributions of fossil fuel, biomass-burning, and biogenic emissions to carbonaceous aerosols in Zurich as traced by 14C, J. Geophys. Res. Atmospheres, 111(D7), D07206, doi:10.1029/2005JD006590, 2006.

Szidat, S., Prévôt, A. S. H., Sandradewi, J., Alfarra, M. R., Synal, H.-A., Wacker, L. and Baltensperger, U.: Dominant impact of residential wood burning on particulate matter in Alpine valleys during winter, Geophys. Res. Lett., 34(5), L05820, doi:10.1029/2006GL028325, 2007.

Szidat, S., Ruff, M., Perron, N., Wacker, L., Synal, H.-A., Hallquist, M., Shannigrahi, A. S., Yttri, K. E., Dye, C. and Simpson, D.: Fossil and non-fossil sources of organic carbon (OC) and elemental carbon (EC) in Göteborg, Sweden, Atmos Chem Phys, 9(5), 1521–1535, doi:10.5194/acp-9-1521-2009, 2009.

Szidat, S., Bench, G., Bernardoni, V., Calzolai, G., Czimczik, C. I., Derendorp, L., Dusek, U., Elder, K., Fedi, M., Genberg, J., Gustafsson, Ö., Kirillova, E., Kondo, M., McNichol, A. P., Perron, N., dos Santos, G. M., Stenström, K., Swietlicki, E., Uchida, M., Vecchi, R., Wacker, L., Zhang, Y. and Prévôt, A. S. H.: Intercomparison of 14C Analysis of Carbonaceous Aerosols: Exercise 2009, Radiocarbon, 55(3–4), doi:10.2458/azu_js_rc.55.16314, 2013.

Uchida, M., Kumata, H., Koike, Y., Tsuzuki, M., Uchida, T., Fujiwara, K. and Shibata, Y.: Radiocarbon-based source apportionment of black carbon (BC) in PM10 aerosols from residential area of suburban Tokyo, Nucl. Instrum. Methods Phys. Res. Sect. B Beam Interact. Mater. At., 268(7–8), 1120–1124, doi:10.1016/j.nimb.2009.10.114, 2010.

Wacker, L., Němec, M. and Bourquin, J.: A revolutionary graphitisation system: Fully automated, compact and simple, Nucl. Instrum. Methods Phys. Res. Sect. B Beam Interact. Mater. At., 268(7–8), 931–934, doi:10.1016/j.nimb.2009.10.067, 2010.

Wacker, L., Fahrni, S. M., Hajdas, I., Molnar, M., Synal, H.-A., Szidat, S. and Zhang, Y. L.: A versatile gas interface for routine radiocarbon analysis with a gas ion source, Nucl. Instrum. Methods Phys. Res. Sect. B Beam Interact. Mater. At., 294, 315–319, doi:10.1016/j.nimb.2012.02.009, 2013.

Waked, A., Favez, O., Alleman, L. Y., Piot, C., Petit, J.-E., Delaunay, T., Verlinden, E., Golly, B., Besombes, J.-L., Jaffrezo, J.-L. and Leoz-Garziandia, E.: Source apportionment of PM10 in a north-western Europe regional urban background site (Lens, France) using positive matrix factorization and including primary biogenic emissions, Atmos Chem Phys, 14(7), 3325–3346, doi:10.5194/acp-14-3325-2014, 2014.

Wise, S. A. and Watters, R. L. J.: National Institute of Standards & Technology. Certificate of Analysis, Standard Reference Material 1649a: Urban Dust, 2007.

Wise, S. A. and Watters, R. L. J.: National Institute of Standards & Technology. Certificate of Analysis, Standard Reference Material 1649b: Urban Dust, 2009.

Yttri, K. E., Dye, C. and Kiss, G.: Ambient aerosol concentrations of sugars and sugar-alcohols at four different sites in Norway, Atmos Chem Phys, 7(16), 4267–4279, 2007.

Zhang, Y. L., Perron, N., Ciobanu, V. G., Zotter, P., Minguillón, M. C., Wacker, L., Prévôt, A. S. H., Baltensperger, U. and Szidat, S.: On the isolation of OC and EC and the optimal strategy of radiocarbon-based source apportionment of carbonaceous aerosols, Atmos Chem Phys Discuss, 12(7), 17657–17702, doi:10.5194/acpd-12-17657-2012, 2012.

Zotter, P., Ciobanu, V. G., Zhang, Y. L., El-Haddad, I., Macchia, M., Daellenbach, K. R., Salazar, G. A., Huang, R.-J., Wacker, L., Hueglin, C., Piazzalunga, A., Fermo, P., Schwikowski, M., Baltensperger, U., Szidat, S. and Prévôt, A. S. H.: Radiocarbon analysis of elemental and organic carbon in Switzerland during winter-smog episodes from 2008 to 2012 – Part 1: Source apportionment and spatial variability, Atmos Chem Phys, 14(24), 13551–13570, doi:10.5194/acp-14-13551-2014, 2014.

X modern carbon	Expected F^{14}C	Standard error [F^{14}C]	Measured F^{14}C (after graphitization)	Standard deviation [F^{14}C]
0	0.0013	0.0001	0.0013	0.0002 (N=5)
0.2	0.2379	0.0185	0.2297	0.0002 (N=3)
0.51	0.6039	0.0131	0.5896	0.0035 (N=3)
0.8	0.9467	0.0096	0.9411	0.0012 (N=3)
1	1.1862	0.0007	1.1862	0.0017 (N=5)

Table 1: Analyses of mixtures of SRM 2975 and SRM 1515 standards in the form of solid graphite targets of large samples (roughly 1 mg C). X modern carbon represents the mass fraction of modern carbon, see Eq. (5). The mass fraction of each SRM can be calculated using their carbon content (i.e. 45% for SRM1 515 and 78 % for SRM 2975). "Expected F^{14}C" is calculated by using the mass of each SRM and its measured F^{14}C as end-members. Measurements are made with solid target (graphitization, roughly 1mgC).

Gaseous source $F^{14}C$	SD (N = 7)	Solid source $F^{14}C$	SD (N = 4)	Literature values $F^{14}C$
0.505	0.028	0.532	0.004	Solid measurement SRM 1649a: 0.523±0.018 (N = 5) (Szidat et al., 2004) 0.507 – 0.61, depending on the sample preparation (Currie et al., 2002; Wise and Watters, 2007) 0.517 / 0.572 (simple /double combustion) (Heal et al., 2011) Solid measurement SRM 1649: 0.61±0.04 (Currie et al., 1984)

Table 2: Analyses of SRM1949b with gaseous and solid (roughly 1 mgC) source. Gaseous measurements are made with punches of loaded quartz filters. Comparison with the literature values for SRM 1649 and SRM 1649a.

Date	PM$_{10}$ [µg. m^{-3}]	Carbon mass [µgC m^{-3}]	± Carbon mass [µgC m^{-3}]	Levoglucosan [µg m^{-3}]	NO$_X$ [µg m^{-3}]	F^{14}C	± F^{14}C	f$_M$	± f$_M$	f$_{NF}$	f$_F$	± f$_F$ / f$_{NF}$
Winter $f_{NF,ref}$ = 1.10 $F^{14}C$ = 1.09 f_M												
24/11/2013	31	15.95	0.46	2.37	Nd	0.986	0.010	0.978	0.010	0.90	0.10	0.02
03/12/2013	***90***	***48.29***	***1.39***	***6.94***	***Nd***	***1.002***	***0.010***	***0.994***	***0.010***	***0.91***	***0.09***	***0.02***
05/12/2013	***60***	***24.56***	***0.73***	***3.50***	***Nd***	***0.977***	***0.011***	***0.970***	***0.011***	***0.89***	***0.11***	***0.02***
06/12/2013	***69***	***37.69***	***1.10***	***5.14***	***Nd***	***1.015***	***0.011***	***1.007***	***0.010***	***0.92***	***0.08***	***0.02***
08/12/2013	***75***	***38.58***	***1.12***	***6.03***	***Nd***	***1.047***	***0.011***	***1.039***	***0.011***	***0.95***	***0.05***	***0.02***
09/12/2013	***93***	***45.87***	***1.33***	***6.26***	***Nd***	***0.969***	***0.010***	***0.962***	***0.010***	***0.88***	***0.12***	***0.02***
12/12/2013	***133***	***53.81***	***1.55***	***7.66***	***177***	***0.987***	***0.010***	***0.979***	***0.010***	***0.90***	***0.10***	***0.02***
13/12/2013	***133***	***57.14***	***1.65***	***8.48***	***170***	***0.985***	***0.010***	***0.977***	***0.010***	***0.90***	***0.10***	***0.02***
15/12/2013	***86***	***34.46***	***1.01***	***5.81***	***68***	***1.067***	***0.011***	***1.059***	***0.011***	***0.97***	***0.03***	***0.02***
16/12/2013	***108***	***42.04***	***1.22***	***6.29***	***145***	***0.964***	***0.010***	***0.956***	***0.010***	***0.88***	***0.12***	***0.02***
18/12/2013	***82***	***28.78***	***0.85***	***4.60***	***120***	***0.926***	***0.010***	***0.919***	***0.010***	***0.84***	***0.16***	***0.02***
20/12/2013	***60***	***25.20***	***0.74***	***4.20***	***81***	***1.003***	***0.011***	***0.995***	***0.010***	***0.91***	***0.09***	***0.02***
01/01/2014	25	7.81	0.23	1.15	25	0.978	0.011	0.971	0.010	0.89	0.11	0.02
22/01/2014	41	17.35	0.50	2.63	57	0.957	0.011	0.949	0.010	0.87	0.13	0.02
12/02/2014	21	7.80	0.23	0.97	34	0.924	0.010	0.917	0.010	0.84	0.16	0.02
13/02/2014	18	6.45	0.20	0.83	23	0.980	0.012	0.972	0.011	0.89	0.11	0.02
15/02/2014	13	3.76	0.12	0.47	13	0.875	0.013	0.868	0.013	0.80	0.20	0.02
16/02/2014	43	16.48	0.48	2.61	32	1.026	0.011	1.018	0.011	0.93	0.07	0.02
19/02/2014	***38***	***17.06***	***0.49***	***2.69***	***Nd***	***0.976***	***0.011***	***0.968***	***0.011***	***0.89***	***0.11***	***0.02***
19/02/2014	***37***	***17.39***	***0.50***	***2.65***	***Nd***	***0.924***	***0.011***	***0.917***	***0.011***	***0.84***	***0.16***	***0.02***
21/02/2014	29	12.06	0.35	1.71	35	1.046	0.011	1.038	0.011	0.95	0.05	0.02
22/02/2014	22	7.08	0.21	0.93	24	1.011	0.011	1.003	0.011	0.92	0.08	0.02
24/02/2014	38	16.17	0.39	2.09	46	0.878	0.008	0.871	0.008	0.80	0.20	0.02
25/02/2014	37	9.81	0.29	1.30	40	0.921	0.011	0.914	0.011	0.84	0.16	0.02
27/02/2014	33	12.37	0.36	1.66	46	0.956	0.011	0.949	0.011	0.87	0.13	0.02
28/02/2014	20	8.81	0.26	1.31	21	1.004	0.011	0.996	0.011	0.91	0.09	0.02
02/03/2014	20	7.25	0.22	1.12	15	1.033	0.011	1.025	0.011	0.94	0.06	0.02
Summer $f_{NF,ref}$ = 1.04 $F^{14}C$ = 1.03 f_M												
28/07/2014	15	3.45	0.11	0.03	14	0.714	0.012	0.708	0.012	0.69	0.31	0.01
30/07/2014	12	2.81	0.10	0.03	17	0.625	0.015	0.620	0.014	0.60	0.40	0.02
31/07/2014	13	3.33	0.11	0.03	11	0.686	0.013	0.680	0.013	0.66	0.34	0.01
02/08/2014	17	3.13	0.11	0.03	10	0.815	0.014	0.809	0.014	0.78	0.22	0.02
03/08/2014	13	2.81	0.10	0.04	6	0.879	0.016	0.872	0.016	0.85	0.15	0.02
05/08/2014	16	3.66	0.12	0.03	11	0.815	0.013	0.809	0.013	0.78	0.22	0.01
06/08/2014	21	4.74	0.15	0.04	15	0.771	0.011	0.765	0.011	0.74	0.26	0.01
08/08/2014	10	3.17	0.11	0.02	14	0.717	0.013	0.711	0.013	0.69	0.31	0.01
09/08/2014	11	3.12	0.10	0.06	11	0.823	0.014	0.816	0.014	0.79	0.21	0.02
11/08/2014	13	2.50	0.09	0.06	13	0.771	0.017	0.764	0.017	0.74	0.26	0.02
12/08/2014	13	2.73	0.10	0.05	10	0.829	0.016	0.822	0.016	0.80	0.20	0.02
14/08/2014	8	1.97	0.08	0.04	9	0.794	0.021	0.788	0.020	0.76	0.24	0.02
15/08/2014	7	2.32	0.09	0.13	9	0.890	0.020	0.883	0.020	0.86	0.14	0.02
17/08/2014	9	2.39	0.09	0.04	7	0.824	0.018	0.817	0.018	0.79	0.21	0.02

Table 3: Results of analysis of Passy samples. PM$_{10}$ is determined by TEOM-FDMS; days with a PM$_{10}$ concentration higher than 50 µg m^{-3} (winter smog) are reported in bold italics (19/02/2014 is sampled with two filters and the sum is greater than 50 µg m^{-3}). Levoglucosan and NO$_X$ concentrations: see text. Carbon concentration is determined using the GIS quantification and is expressed with its confidence interval. Each radiocarbon value (expressed in F^{14}C and f$_M$) is based on duplicated measurements: here the weighted mean and its weighted error (2σ i.e. 95 % confidence interval) is presented. For winter, it is considered that all the non-fossil carbon originates from biomass burning (i.e. f$_{NF,ref}$= F^{14}C$_{bb}$) whereas all the non-fossil carbon during summer is assumed to originate from biogenic emissions (i.e. f$_{NF,ref}$= F^{14}C$_{bio}$). The reference values (f$_{NF,ref}$) for winter and summer are expressed in F^{14}C f$_M$. Fossil and non-fossil fractions (f$_F$ and f$_{NF}$) are determined by the radiocarbon measurements (see Eq. (6)).

Date	PM_{10} [µg m^{-3}]	Carbon mass [µgC m^{-3}]	± Carbon mass [µgC m^{-3}]	Levoglucosan [µg m^{-3}]	NO_X [µg m^{-3}]	$F^{14}C$	± $F^{14}C$	f_M	± f_M	f_{NF}	f_F	± f_F / f_{NF}
05/12/2013	44	19.75	0.57	2.66	174	0.900	0.011	0.893	0.011	0.82	0.18	0.02
08/12/2013	44	24.80	0.73	3.83	129	1.017	0.012	1.009	0.012	0.92	0.08	0.02
11/12/2013	***63***	***29.52***	***0.87***	***3.87***	***250***	***0.872***	***0.010***	***0.865***	***0.010***	***0.79***	***0.21***	***0.02***
14/12/2013	40	20.97	0.60	3.23	133	0.968	0.011	0.961	0.011	0.88	0.12	0.02
17/12/2013	***53***	***29.97***	***0.88***	***3.45***	***263***	***0.865***	***0.011***	***0.858***	***0.011***	***0.79***	***0.21***	***0.02***
20/12/2013	18	7.08	0.21	0.87	74	0.841	0.011	0.834	0.011	0.76	0.24	0.02
23/12/2013	39	20.09	0.60	3.02	170	0.914	0.011	0.907	0.011	0.83	0.17	0.02
26/12/2013	14	5.73	0.18	0.79	57	0.918	0.012	0.911	0.011	0.83	0.17	0.02
29/12/2013	18	8.36	0.25	1.17	67	0.943	0.013	0.935	0.013	0.86	0.14	0.02
01/01/2014	***61***	***26.29***	***0.77***	***4.21***	***154***	***1.018***	***0.012***	***1.010***	***0.012***	***0.93***	***0.07***	***0.02***
04/01/2014	17	8.48	0.25	1.23	82	0.942	0.011	0.934	0.011	0.86	0.14	0.02
07/01/2014	36	19.83	0.57	2.86	161	0.897	0.011	0.890	0.011	0.82	0.18	0.02

Table 4: Results of analysis of Chamonix samples. PM_{10} is determined by TEOM-FDMS; days with a PM_{10} concentration higher than 50 µg m^{-3} (winter smog) are reported in bold italic. Levoglucosan and NO_X concentrations: see text. Carbon concentration is determined using the GIS quantification and is expressed with its confidence interval. Each radiocarbon value (expressed in $F^{14}C$ and f_M) is based on duplicated measurements: here the weighted mean and its weighted error (2σ i.e. 95 % confidence interval) is presented. Fossil and non-fossil fractions (f_F and f_{NF}) are determined by the radiocarbon measurements (see Eq. (6)).

	TC_{NF} vs. Levoglucosan					**TC_F vs. NO_X**				
	a	±a	b	±b	Pearson's R	a	±a	b	±b	Pearson's R
Passy Summer p_{bio} = 1	-	-	-	-	-	0.103	0.012	-0.366	0.124	0.822
Passy Summer p_{bio} = 0.4	-	-	-	-	-	0.099	0.014	-0.270	0.145	0.813
Passy Summer p_{bio} = 0.2	-	-	-	-	-	0.100	0.014	-0.259	0.145	0.809
Passy Summer p_{bio} = 0	-	-	-	-	-	0.107	0.013	-0.284	0.132	0.806
Passy Winter p_{bio} = 1	6.33	0.20	0.38	0.29	0.995	0.024	0.002	-0.040	0.063	0.782
Passy Winter p_{bio} = 0.4	6.11	0.20	0.38	0.30	0.995	0.028	0.004	0.127	0.134	0.914
Passy Winter p_{bio} = 0.2	6.04	0.20	0.37	0.30	0.995	0.031	0.004	0.129	0.133	0.935
Passy Winter pbio = 0	5.98	0.19	0.36	0.28	0.995	0.036	0.003	0.062	0.086	0.950
Chamonix Winter p_{bio} = 1	6.29	0.35	0.12	0.54	0.989	0.019	0.002	-0.490	0.167	0.885
Chamonix Winter p_{bio} = 0.4	6.06	0.35	0.13	0.55	0.989	0.021	0.003	-0.392	0.283	0.938
Chamonix Winter p_{bio} = 0.2	6.00	0.35	0.13	0.54	0.989	0.023	0.003	-0.407	0.283	0.949
Chamonix Winter p_{bio} = 0	5.94	0.33	0.12	0.51	0.989	0.024	0.002	-0.467	0.213	0.959

Table 5: Determination of the linear fit parameters (with their 95% confidence intervals) for the linear relation between TC_{NF} and levoglucosan, and for the linear relation between TC_F and NO_X. Variation in p_{bio} and in TC_{NF} and TC_F does not have a major influence on the regression parameters in the case of "TC_{NF} vs. Levoglucosan" but does in the case of "TC_F vs. NO_X" because of the small amount of TC_F.

Date	TC$_{bb}$ [µgC m^{-3}]	± TC$_{bb}$ [µgC m^{-3}]	TC$_{bio}$ [µgC m^{-3}]	± TC$_{bio}$ [µgC m^{-3}]	TC$_{F}$ [µgC m^{-3}]	± TC$_{F}$ [µgC m^{-3}]	TC$_{NF}$/TC	TC$_{F}$/TC	TC$_{bio}$/TC$_{NF}$	polyol [ng m^{-3}]	± polyol [ng m^{-3}]
28/07/2014	0.18	0.02	2.18	0.09	1.09	0.15	0.68	0.32	0.92	64.56	6.46
30/07/2014	0.21	0.02	1.47	0.08	1.14	0.12	0.60	0.40	0.88	79.88	7.99
31/07/2014	0.21	0.02	1.98	0.09	1.15	0.14	0.66	0.34	0.90	74.04	7.40
02/08/2014	0.18	0.02	2.26	0.10	0.69	0.14	0.78	0.22	0.92	80.91	8.09
03/08/2014	0.26	0.03	2.10	0.10	0.45	0.14	0.84	0.16	0.89	80.23	8.02
05/08/2014	0.19	0.02	2.67	0.11	0.80	0.16	0.78	0.22	0.93	65.20	6.52
06/08/2014	0.25	0.03	3.25	0.13	1.24	0.20	0.74	0.26	0.93	55.61	5.56
08/08/2014	0.14	0.02	2.03	0.09	1.00	0.14	0.69	0.31	0.93	85.26	8.53
09/08/2014	0.36	0.04	2.09	0.10	0.67	0.15	0.78	0.22	0.85	76.51	7.65
11/08/2014	0.38	0.04	1.45	0.09	0.67	0.13	0.73	0.27	0.79	62.80	6.28
12/08/2014	0.27	0.03	1.89	0.09	0.57	0.14	0.79	0.21	0.87	94.51	9.45
14/08/2014	0.25	0.03	1.24	0.08	0.48	0.11	0.76	0.24	0.83	50.09	5.01
15/08/2014	0.76	0.08	1.19	0.12	0.38	0.17	0.84	0.16	0.61	45.14	4.51
17/08/2014	0.25	0.03	1.63	0.09	0.51	0.13	0.79	0.21	0.87	38.93	3.89

Table6: Results of summer samples from Passy. TC$_{bb}$ is calculated from levoglucosan concentration. TC$_{bio}$ and TC$_{F}$ come out from TC$_{bb}$ and the F^{14}C of the sample. TC$_{NF}$/TC and TC$_{F}$/TC are equivalent to f$_{NF}$ and f$_{F}$ determined directly by ^{14}C measurements. The major part of TC$_{NF}$ is composed of TC$_{bio}$. The uncertainties represent the confidence intervals (95 %), and are determined by uncertainties propagation.

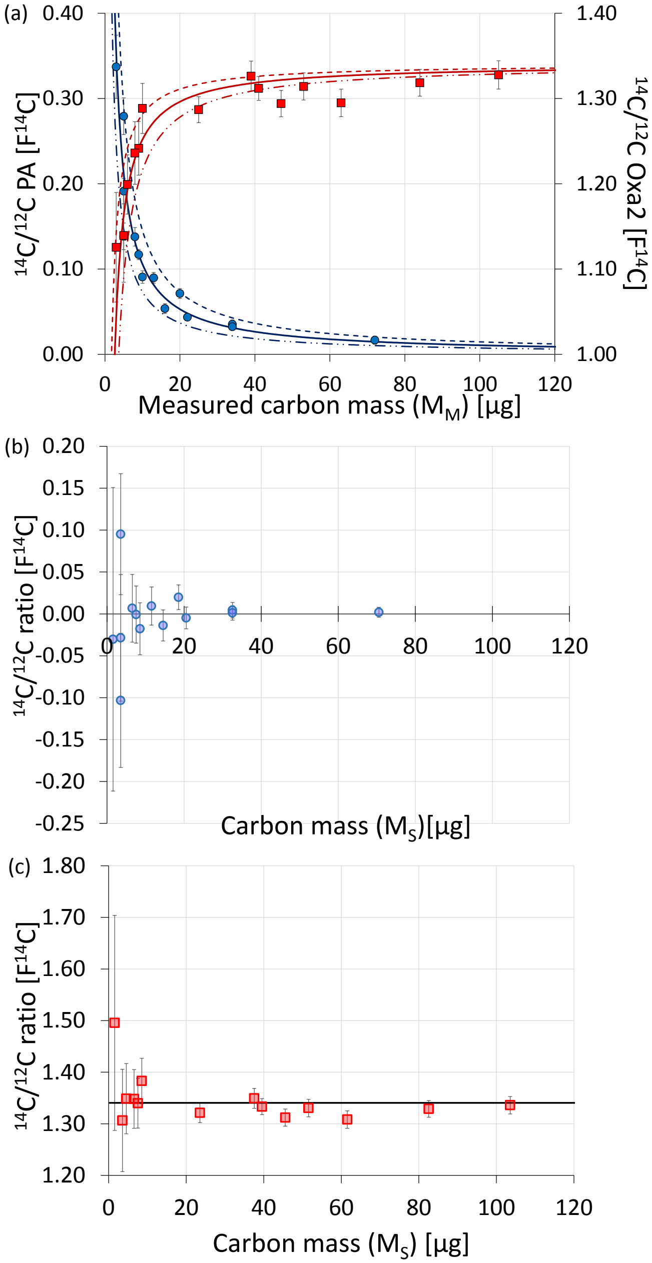

Figure 1: Measurements and corrections for blank (phthalic acid, PA) and standard (oxalic acid 2, OxA2) samples. (a) Blue dots represents the measured ^{14}C/^{12}C ratio for sample blanks and red dots stand for standard measurements. Solid lines and dashed lines represent the least square optimization with its 95% confidence interval. M_M is the measured carbon mass. (b) Blue dots are the corrected blank measurements. M_S is the sample carbon mass (i.e. the measured carbon mass corrected for the contaminant carbon mass) (c) Red squares are the corrected standard measurements, the line at 1.3406 stands for the certified value of OxA2. M_S is the sample carbon mass (i.e. the measured carbon mass corrected for the contaminant carbon mass). The results shown in (b) (blank) and (c) (standard) illustrate the quality of the correction.

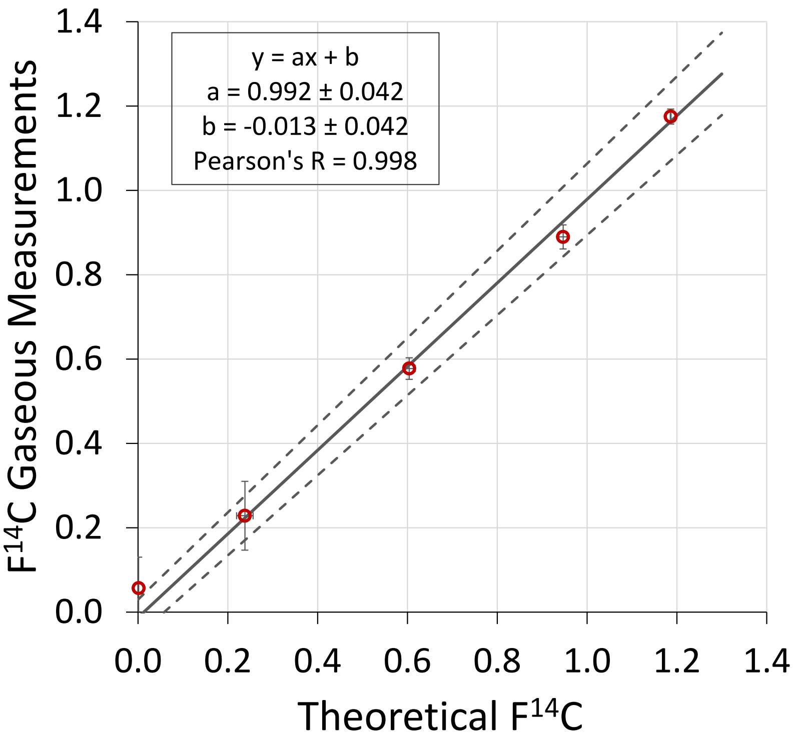

Figure 2: F^{14}C values of synthetic and standard (test) aerosol samples measured with the gas source compared with theoretical values. These test aerosols are made of two Standard Reference Materials (SRM 2975 and SRM 1515). The compositions of the different mixtures are listed in Table 1 with the corresponding theoretical and measured F^{14}C. The coefficients of the linear regression have been calculated by taking into account error bars (2 SD) on both axes and are given with their 95 % confidence interval. The linear relation confirms the accuracy of aerosol measurements with the gas ion source over the full range of expected ^{14}C activities.

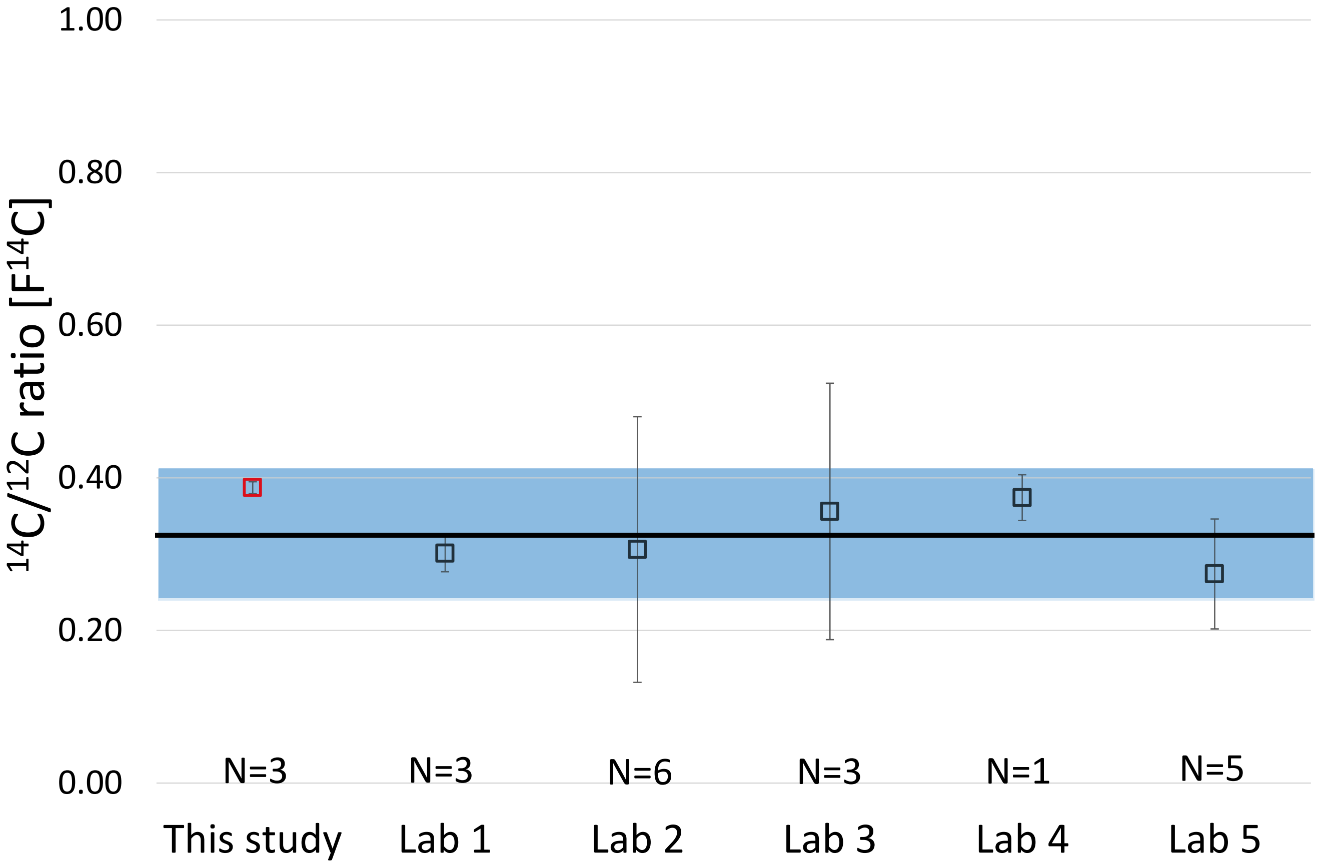

Figure 3: RM 8785 measurements. Black squares and error bars represent values and measurements uncertainties at 2σ, described in Szidat et al. (2013). The black line stands for the average value and the blue ribbon represents the 2σ confidence interval for Labs 1-5. The red square shows the weighted average result obtained for this study (N = 3) and its weighted error (2σ). The large scatter could be linked to heterogeneous loading during the production of RM 8785 as mentioned by Cavanagh and Watters (2005). The value obtained in this study is compatible with the high end of measurements performed by the five different laboratories.

Figure 4: Location of the sampling stations in the Arve valley investigated in this study. PM was sampled between November 2013 and August 2014 in Passy and between December 2013 and January 2014 in Chamonix. Both are urban stations, collecting the PM$_{10}$ fraction of atmospheric aerosols.

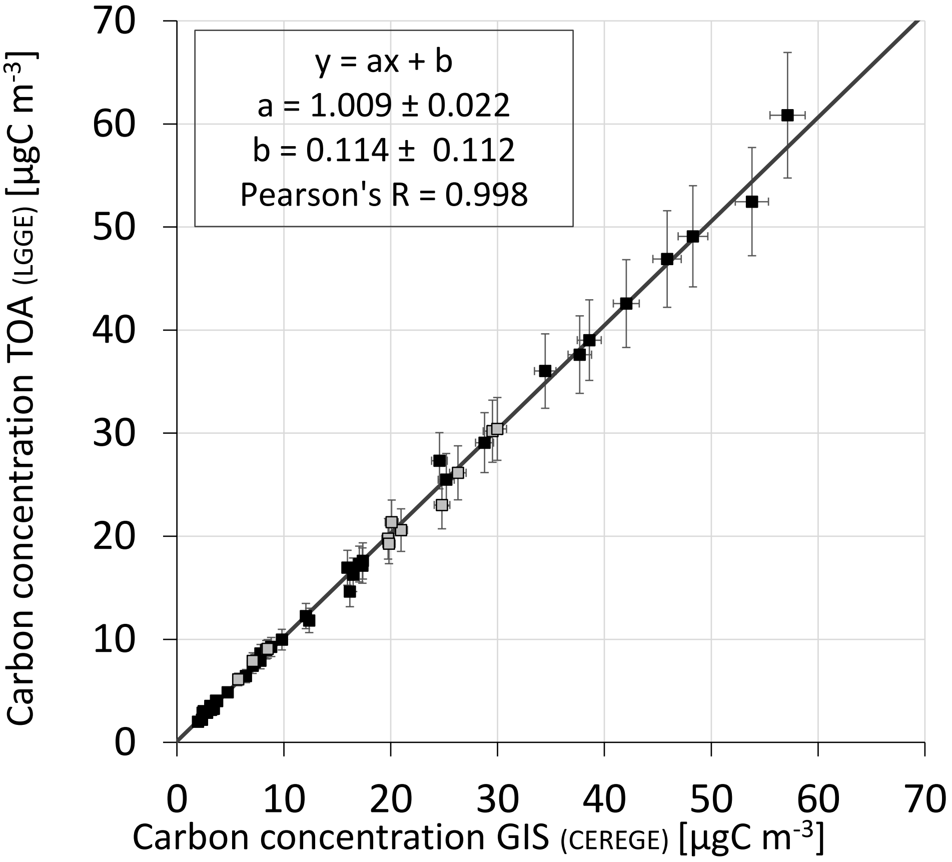

Figure 5: Total carbon concentration measurements. Comparison between TOA (LGGE in Grenoble) and GIS (CEREGE in Aix-en-Provence) measurements. The grey squares stand for the Chamonix samples and the black squares stand for the Passy samples. The regression parameters, given with their 95 % confidence intervals, have been calculated by taking into account error bars on both axes and exhibit a very good correlation between the two carbon concentrations; the two sets of measurements can be considered as equivalent.

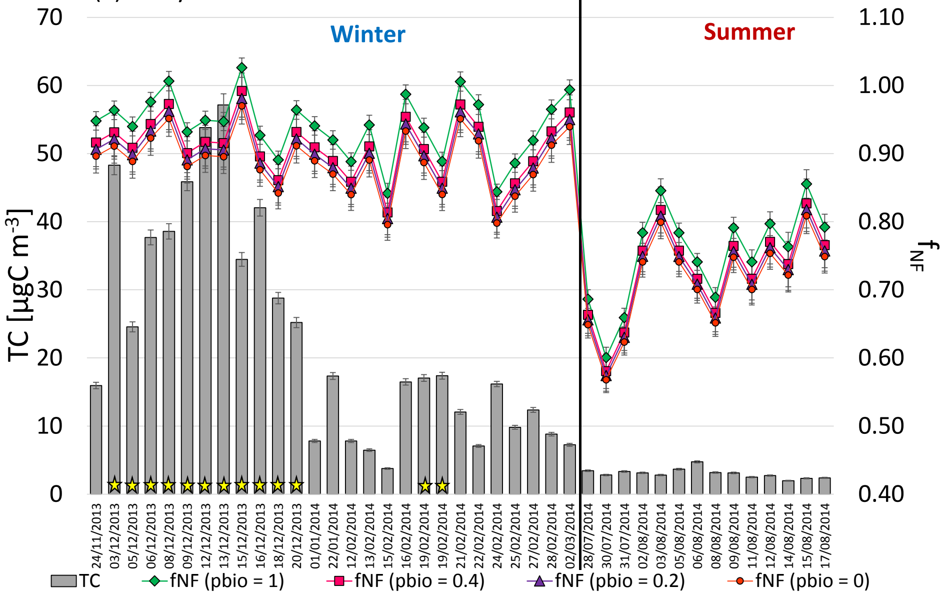
(a) Passy

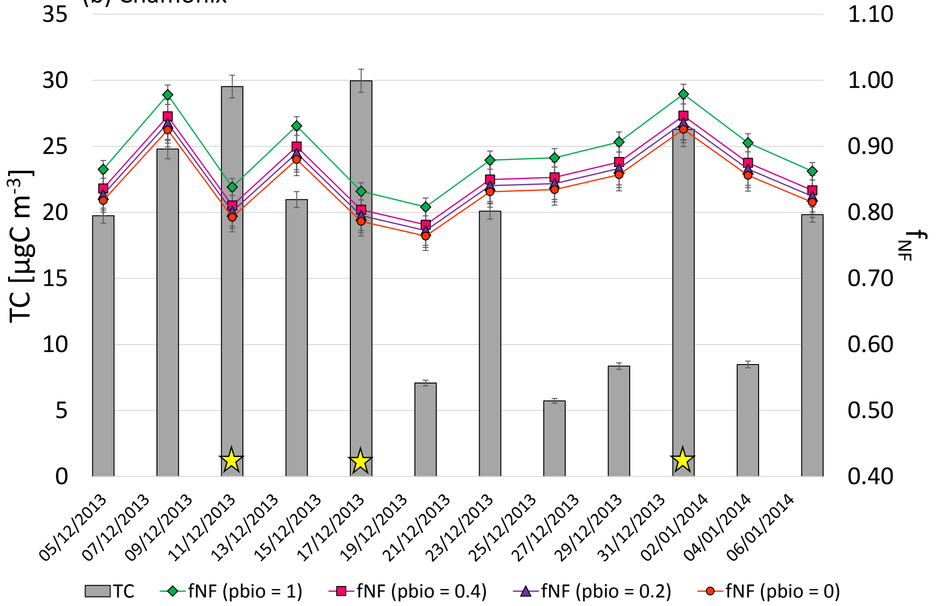
(b) Chamonix

Figure 6: Results for (a) Passy and (b) Chamonix. Grey bars represent carbon concentration. Days with a PM$_{10}$ concentration higher than 50 µg m^{-3} are marked with a yellow star. Green diamonds stand for the only biogenic f$_{NFref}$, pink squares are for f$_{NFref}$ with a 40 % biogenic fraction, purple triangles denote f$_{NFref}$ with a 20% biogenic fraction and red dots stand for f$_{NFref}$ with a 0% biogenic fraction. In both case, the non-fossil fraction remains at very high levels during the winter season, validating the importance of the non-fossil source. A maximum variation of 6 % is observed in the different f$_{NF}$ estimations.

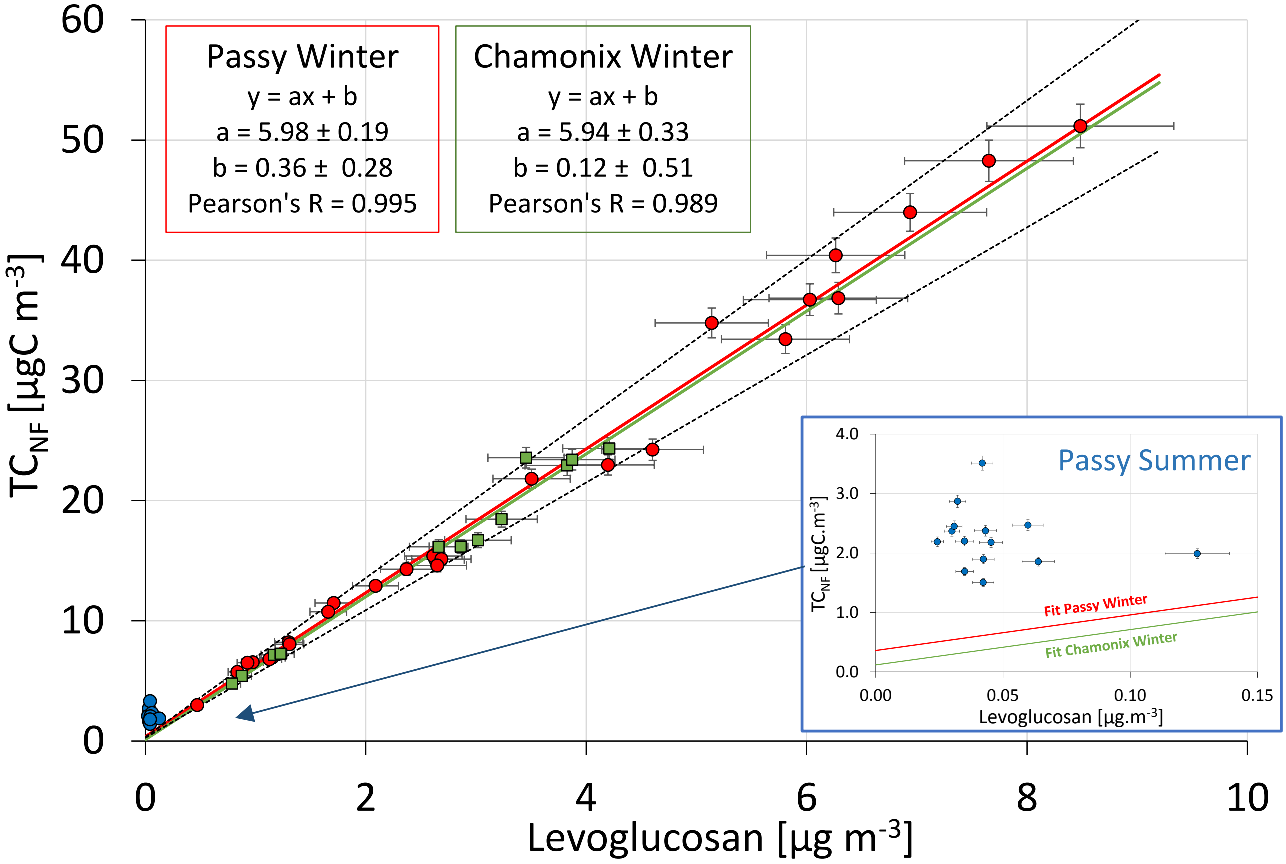

Figure 7: Comparison of TC$_{NF}$, based on $^{14}C/^{12}C$ ratio measurements, with levoglucosan. TC$_{NF}$ corresponds to the carbon concentration multiplied by the f$_{NF}$. For the winter sample, f$_{NF}$ is determined for p$_{bio}$ = 0 and for summer samples, p$_{bio}$ = 1. It has to be underlined that a variation in p$_{bio}$ does not affect the significance of the relationship between levoglucosan and TC$_{NF}$ (see Table 5). Green squares indicate Chamonix winter samples, red dots Passy winter samples and blue dots denote Passy summer samples. Winter samples display very strong correlations between TC$_{NF}$ and levoglucosan with close to zero intercepts suggesting that virtually all of the TC$_{NF}$ originates from biomass burning. The fit parameters have been calculated by taking into account both error bars on the x and y axes and are given with their 95 % confidence interval. Black dotted lines stand for two extreme cases assuming only young air (i.e. SOA = 25 % of POA) or only older air (i.e. SOA = 50 % of POA), see Sect. 3.2.1. for further informations. No correlation is found for the summer samples, implying the summer TC$_{NF}$ originate from other non-fossil sources.

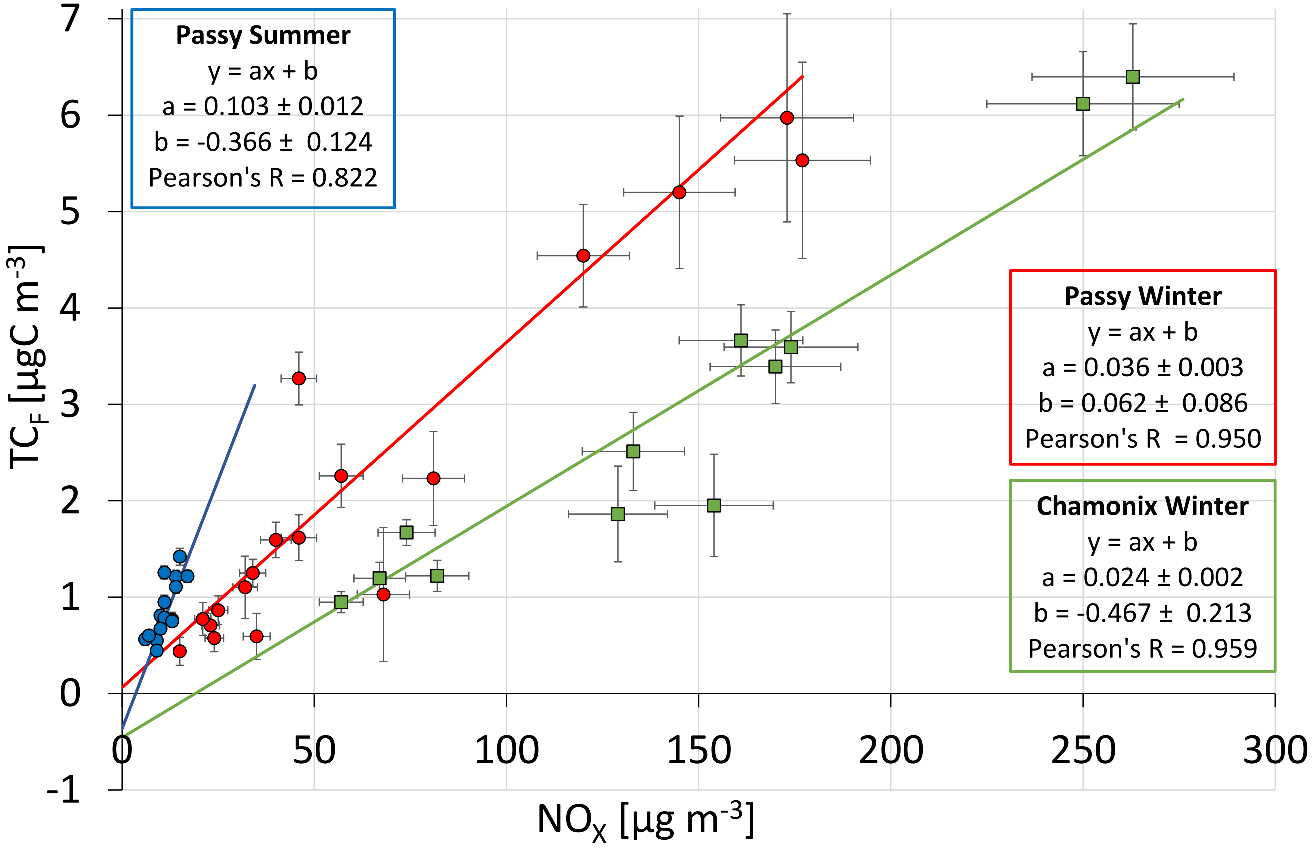

Figure 8: Comparison of TC_F, based on $^{14}C/^{12}C$ ratio measurements, with NO_X. TC_F corresponds to the carbon concentration multiplied by f_F. For the winter sample, f_F is determined for $p_{bio} = 0$ and for summer samples, $p_{bio} = 1$. It has to be underlined that a variation in p_{bio} does not affect the significance of the relationship between levoglucosan and TC_{NF} (see Table 5). Green squares denote Chamonix winter samples, red dots Passy winter samples and blue dots designate Passy summer samples. Each data set exhibits a good correlation between NO_X and TC_F concentrations. The fit parameters have been calculated by taking into account both error bars on the x and y axes and are given with their 95 % confidence interval. A higher slope value is obtained for the summer data set than for the winter ones, which suggests either different fossil carbon sources or NO_X degradation rate depending on the season.

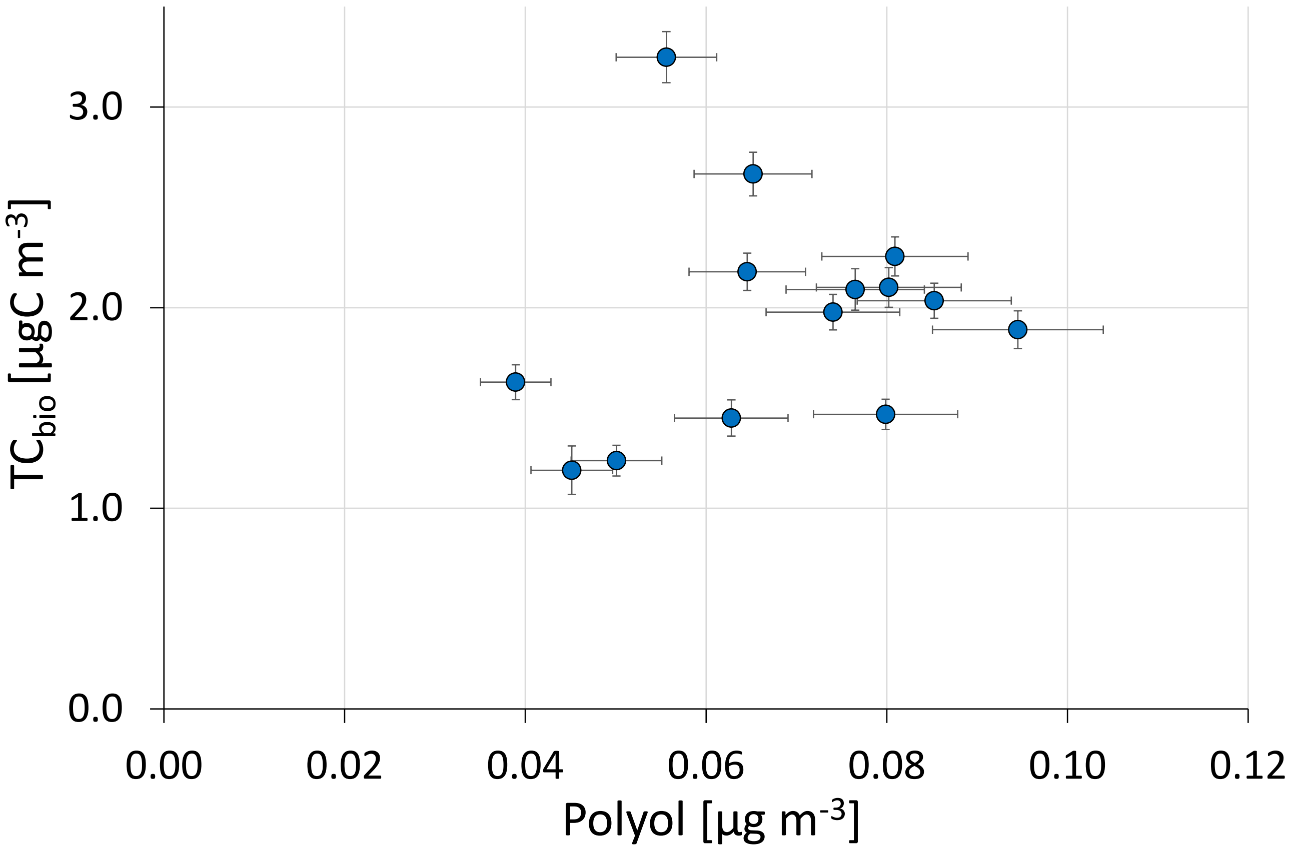

Figure 9: Comparison of TC_{bio}, based on levoglucosan and $^{14}C/^{12}C$ ratio measurements against polyol concentrations. Blue dots stand for the Passy summer samples. No correlation is found between TC_{bio} and polyols concentrations (primary biogenic emissions tracers). TC_{bio} could originate from secondary organic carbon from the oxidation of biogenic VOC.

5

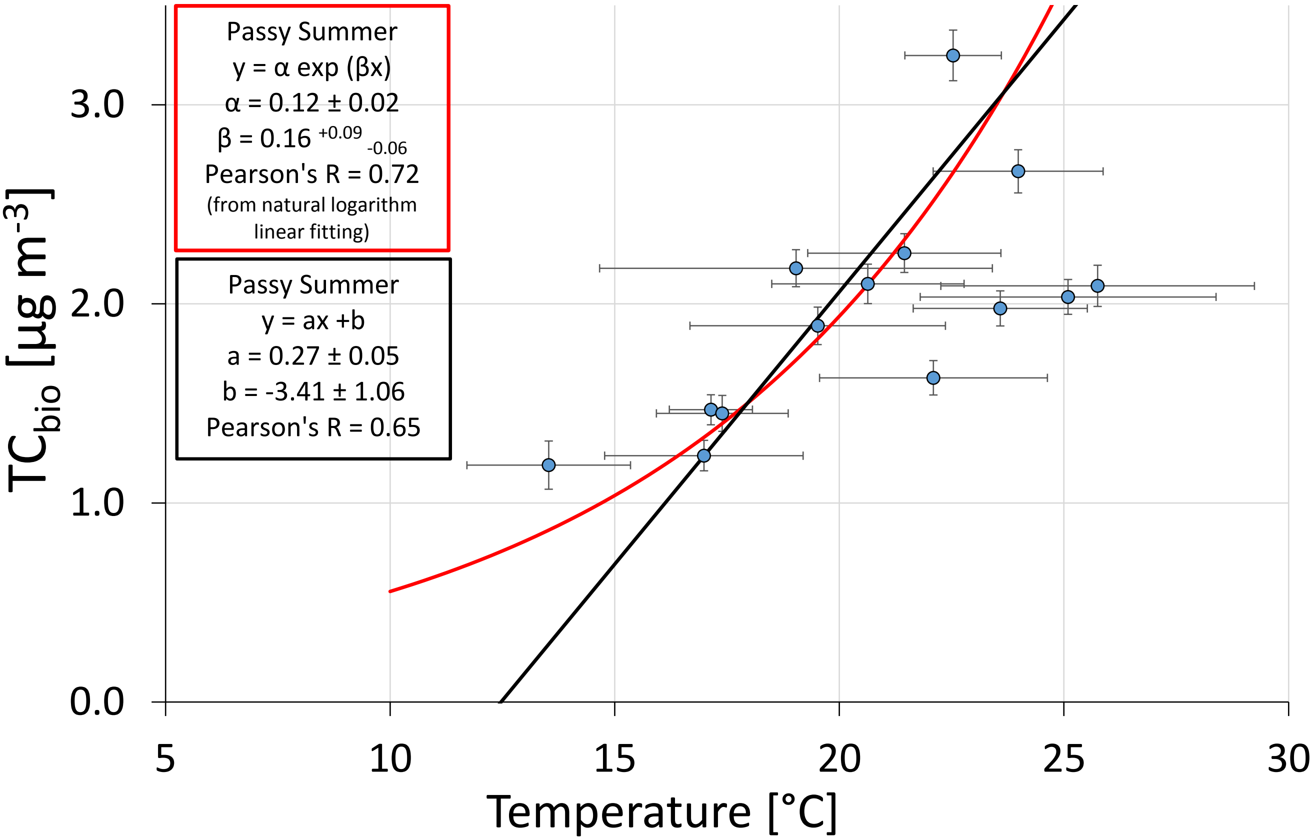

5 **Figure 10: Comparison of TC_{bio}, based on levoglucosan and $^{14}C/^{12}C$ ratio measurements plotted versus the average temperature of the warmest part of the day (10 am to 6 pm). Blue dots stand for the Passy summer samples. TC_{bio} concentration increases with the temperature. Both linear (black line) and exponential (red line) relations are represented with their correlation coefficient. The fit parameters have been calculated by taking into account both error bars on the x and y axes and are given with their 95 % confidence interval. The exponential fit is preferred as the TC_{bio} emission cannot be negative. Moreover, emission of BVOCs (precursors of SOA) emission rate is classically described with an exponential law (Leaitch et al., 2011).**